Historical Trends and Future Projections of Key Performance Parameters in Aircraft Design

Huseyin Acar*, Maxfield Arnson[†], Michael Tsai[‡], and Gokcin Cinar[§¶]

Department of Aerospace Engineering, University of Michigan, Ann Arbor, Michigan 48109

This study presents a comprehensive analysis of historical trends and future projections for key performance parameters (KPPs) in commercial turbofan aircraft, focusing on operational empty weight to maximum takeoff weight ratio (OEW/MTOW), thrust-to-weight ratio (T/W), thrust-specific fuel consumption (TSFC), and lift-to-drag ratio (L/D). Leveraging an extensive dataset of over 400 commercial aircraft and 200 engines, compiled from authoritative sources such as FAA and EASA certifications, along with enhanced regression modeling, this study systematically examines the evolution of each KPP in response to technological advancements, market demands, and regulatory constraints. The analysis reveals that while TSFC improvements align closely with technological advances in engine efficiency, trends in OEW/MTOW, T/W, and L/D reflect complex interactions among performance requirements and aircraft mission profiles. Projections suggest that further gains in these parameters may be limited within conventional aircraft configurations. This work lays a robust foundation for the open-source Future Aircraft Sizing Tool (FAST), equipping designers with data-driven insights to support early-stage design decisions and providing a transparent resource for understanding the historical and technical drivers of commercial aircraft performance.

Nomenclature

α	=	Installed Thrust Lapse
AR	=	Aspect Ratio
C	=	Thrust Specific Fuel Consumption
C_{D0}	=	Coefficient of drag at zero lift
C_{DR}	=	Coefficient of additional drags
D	=	Drag

*Graduate Student, Department of Aerospace Engineering, University of Michigan, Ann Arbor, Michigan 48109.

[†]Graduate Student, Department of Aerospace Engineering, University of Michigan, Ann Arbor, Michigan 48109, AIAA Student Member.

[‡]Research assistant, Department of Aerospace Engineering, University of Michigan, Ann Arbor, Michigan 48109.

[§]Assistant Professor, Department of Aerospace Engineering, University of Michigan, Ann Arbor, Michigan 48109, AIAA Senior Member.

[¶]Corresponding author. Email: cinar@umich.edu

k	=	Growth Rate
K_1	=	Coefficient in lift-drag polar equation
K_2	=	Coefficient in lift-drag polar equation
L	=	Lift
L/D	=	Lift-to-drag ratio
La	=	Lower Asymptote
MAC	=	Mean Aerodynamic Chord
M_0	=	Cruise Mach Number
MTOW	=	Maximum Takeoff Weight
$\dot{m}_f$	=	Fuel mass flow rate
n	=	Load Factor
OEW	=	Operational Empty Weight
OPR	=	Overall Pressure Ratio
P_s	=	Weight-specific excess power
q	=	Dynamic Pressure
R	=	Range
Re_{mac}	=	Mean Aerodynamic Chord Reynolds Number
S	=	Wing Area
T	=	Maximum Takeoff Thrust
TET	=	Turbine Entry Temperature
θ	=	Cruise to sea-level temperature ratio
τ	=	Inflection point
TSFC	=	Thrust Specific Fuel Consumption
U	=	Upper Asymptote
V	=	Velocity
W	=	Weight
W_0	=	Gross Weight
W_{Empty}	=	Empty Weight
W_f	=	Final Weight
W_{Fuel}	=	Fuel Weight
W_i	=	Initial Weight
$W_{payload}$	=	Payload Weight

W/S	=	Wing Loading
β	=	Instantaneous Weight Fraction
η_{tot}	=	Overall Engine Efficiency

I. Introduction

The aviation industry has witnessed significant advancements in aircraft design, driven by evolving technological capabilities and market demands. This paper methodically analyzes historical trends in key performance parameters (KPPs) of aircraft and projects these trends into the future.

Contemporary aircraft design methodologies, as presented in renowned references such as Raymer [1], Roskam [2], and Torenbeek [3], often utilize regressions based on historical data for various aircraft categories. After determining the requirements of the designed aircraft, top-level metrics such as the initial weight fraction and thrust-to-weight ratio are predicted from the parameters of similar aircraft. However, the data underpinning these regressions often lack transparency, accessibility, and clarity in assumptions. For instance, a single aircraft can have multiple weight variations due to different configurations or modifications, yet how such variations are accounted for in the regressions is often ambiguous. Furthermore, these regressions may not capture how these parameters are affected by component-level technological advancements over time.

Several studies have investigated the historical evolution of aircraft performance parameters, though limitations in data transparency and scope are evident. Martinez et al. [4] conducted an extensive analysis using data from 73 jet engines and 116 propeller-driven airplanes to trace the evolution of aircraft performance. Despite the large dataset, this study lacked transparency in data collection and did not clearly address variations in weight. Similarly, Lee [5] examined trends in thrust specific fuel consumption (TSFC), lift-to-drag ratio (L/D), and the operational empty weight to maximum takeoff weight ratio (OEW/MTOW) to assess potential emission reductions in aviation. However, the analysis was constrained by the limited number of aircraft—just 31—considered in the study, which may not fully represent historical evolution. Ballal and Zelina [6] extended this investigation to include aeroengine specifications from 1938 to 2003 across both military and civil aircraft, yet the specific engines analyzed were not clearly identified.

A recurring issue in these studies is the lack of direct publication of certain key parameters, such as L/D, by authorized sources, necessitating their estimation through indirect methods. This often leads to inconsistencies in historical analyses. For instance, some studies, like Martinez et al. [7], estimate L/D without detailing the underlying parameters, while others like Lee [5] provide L/D values but fail to cite clear data sources. As a result, Martinez and Perez [8] reported a 50% increase in L/D over time, whereas Lee et al. [9] observed only a 15% improvement, highlighting the variability in conclusions drawn from different methodologies [10].

The literature also often overlooks the interdependencies between various performance parameters, focusing narrowly on individual metrics. For example, analyzing changes in OEW/MTOW as an indicator of structural efficiency requires considering how aircraft size and range capabilities have evolved. Without acknowledging these interactions, studies may underestimate the impact of advances in materials and composite technologies on structural efficiency.

This study aims to address these limitations by conducting a comprehensive analysis of selected performance parameters across a wide range of aircraft. By providing future projections, this research offers insights that may support further studies on cost and emission reduction strategies in the years ahead. It highlights the necessity of a holistic approach to parameter analysis, demonstrating that a more detailed understanding of the evolution of performance parameters is essential for accurate forecasting and effective design innovation.

This study stands apart by examining a comprehensive database of over 400 aircraft, spanning diverse sizes and entry-into-service (EIS) years. This database, constructed from publicly available information from trusted sources such as manufacturer's technical specifications sheets, airport planning manuals (APM), and type certificate data sheets (TCDS) published by the Federal Aviation Administration (FAA) and the European Union Aviation Safety Agency (EASA), offers a transparent view of the evolution of aircraft KPPs. By correlating these parameters with underlying physical phenomena, the study aims to provide a more profound understanding of the observed trends.

An important outcome of this research is the development of the Future Aircraft Sizing Tool (FAST) [11], an open-source software that leverages the historical trends analyzed in this paper. Developed as part of NASA's Electrified Powertrain Flight Demonstrators (EPFD) project, FAST relies on the historical trends and projections of KPPs to generate initial aircraft designs with minimal input, allowing for rapid exploration and estimation. At the same time, it is flexible enough to incorporate physics-based models or more detailed data when available. Although this paper does not detail the construction of FAST, it serves as the foundation for the tool by offering a comprehensive analysis of the historical data that underpins its predictive capabilities.

The insights from this research are intended for aircraft designers and researchers. While rooted in historical data, projecting future trends inherently carries uncertainties. However, with a clear understanding of past trends and their drivers, stakeholders can make informed decisions for future aircraft designs, ensuring alignment with technological progress and market requirements.

Following this introduction, the selection of KPPs, data collection, and historical trend analysis in the technical approach are discussed. The subsequent section provides historical trends, identifies underlying drivers, and makes informed projections for the future.

II. Technical Approach

A. Selection of Key Performance Parameters (KPPs)

Key performance parameters are critical in the early stages of aircraft design, offering a foundational set of variables that dictate performance and sizing. Initially, KPPs are defined as abstract yet essential elements that support high-level aircraft modeling, sizing, and performance assessments. These parameters are selected to provide an appropriate level of abstraction suitable for the conceptual design stage. For example, the Breguet Range Equation (BRE), given in Eq. 1, a cornerstone for estimating aircraft performance, utilizes high-level performance parameters integral to aerodynamic efficiency (through L/D), propulsion system efficiency (through $TSFC$, or in short, C), performance (through V), and the aircraft weight ratio (through W_i/W_f).

$$R = \frac{V}{C}\frac{L}{D}\ln\left(\frac{W_i}{W_f}\right) \tag{1}$$

Despite its simplicity, the BRE is a powerful tool for early-stage analysis because it provides valuable insights with minimal data requirements. However, as the aerospace industry explores disruptive technologies, such as those with electrified propulsion, the traditional BRE faces limitations in accurately estimating performance due to the distinct characteristics of these new propulsion systems. Expanding upon this conventional approach, Jansen and Duffy [12–14] identified and applied new KPPs to extend the BRE to Electrified Aircraft Propulsion (EAP) systems. They introduced modifications that account for the efficiency and weight of the turboelectric drive, allowing for a more nuanced assessment of aircraft performance. Their work categorizes KPPs into parameters that directly correlate with aircraft aerodynamics, structures, propulsion, and *power*—a distinction not separately made in the BRE—laying a foundation for a generalized parameter space that encompasses both conventional and electrified aircraft propulsion concepts.

Acknowledging the contributions of several authors who have identified historical trends and future projections in electric powertrain-specific components, this paper fills in the remaining KPPs. Specifically, Pastra et al. [15] explore future projections for the specific power and efficiency of electric machines (EMs) used in aircraft, Hall et al. [16] project the specific power and efficiency of power converters through the year 2050, and Tiede et al. [17] make specific energy projections for electric aircraft

In this study, the focus is predominantly on conventional KPPs—OEW/MTOW, T/W, L/D, and TSFC—due to their significance in representing various facets of aircraft performance: structural efficiency, aerodynamic efficiency, and propulsion efficiency. While the list of KPPs can be expanded, our approach emphasizes the importance of making informed estimates with a limited set of data, particularly when designing innovative and unconventional aircraft.

B. Data Collection Approach

Historical data serves as a foundational element for forecasting future trends in aircraft and engine KPPs. To ensure reliable projections, a substantial database was required. However, many existing databases often lack source citations and seldom offer the level of specificity needed for the intended analysis. For instance, Roux published two books on turbofan and turboprop engines in 2007 and 2011 respectively [18, 19]. These books are comprehensive, however they only provide information on engines, not aircraft themselves, and do not include contemporary designs. Additionally, the data books are not formatted for easy digital manipulation. Janes *All The World's Aircraft* [20] is a large aircraft database, although it is not free to use. The FAA [21], Eurocontrol [22], and Jenkinson et al. [23] have publicly available databases online, however these are not comprehensive, including small sample sets of aircraft data.

To address these shortcomings, this study initiated the compilation of a specialized database, encompassing over 400 commercial aircraft and more than 200 turbofan engines, supplemented by a selection of turbojet engines. This database integrates aircraft and engine data to delineate a complete profile of each vehicle.

The primary sources for data collection were TCDS published online by the FAA, EASA, the United Kingdom's Civil Aviation Authority (CAA), and other government aviation authorities. The TCDS data was enriched with information from aircraft manufacturer brochures and websites, airport planning manuals, and manufacturer CAD models. Similarly, engine data was gathered from TCDS and various data handbooks.

C. Data Structure and Analytical Application in FAST

The data used in this study is publicly available within the FAST repository [11] and can be accessed as either either structured MATLAB files or spreadsheets to support reproducibility in various programs such as JMP. For streamlined organization and analysis in MATLAB, the data is hierarchically structured as a MATLAB 'struct', as illustrated in Fig. 1. Each aircraft entry in the database contains over 100 parameters detailing various aspects of both the vehicle and its engines. In this structure, "leaves" at the endpoints represent specific parameter values, while "branches" categorize these parameters into broader classifications. Ellipses are shown under an element in Fig. 1 if additional elements are in the same group but omitted for brevity. For example, the two main branches, "specifications" (specs.) and "overview," connect to sub-branches for "performance," "propulsion," "weight," and others, allowing efficient data retrieval.

This paper sets the foundation for further predictive analysis within the FAST framework by identifying essential physical relationships in the aircraft data. Building on these foundational insights, Arnson et al. [24] later applied probabilistic regressions to the same dataset, incorporating as much design information as possible to improve upon traditional regression models by Raymer, Roskam, and Jenkinson. This paper examines correlations between entry-into-service (EIS) year and parameters such as OEW and T/W, concluding that EIS alone is an unreliable predictor of OEW-to-MTOW ratios due to OEW's dependence on mission-specific design requirements rather than purely technological advancements. By analyzing these trends, the current study establishes the physical relationships that inform which parameters are most relevant in predicting unknown values during the conceptual design phase—insights that have since been used to guide the regression models in Arnson et al.'s work.

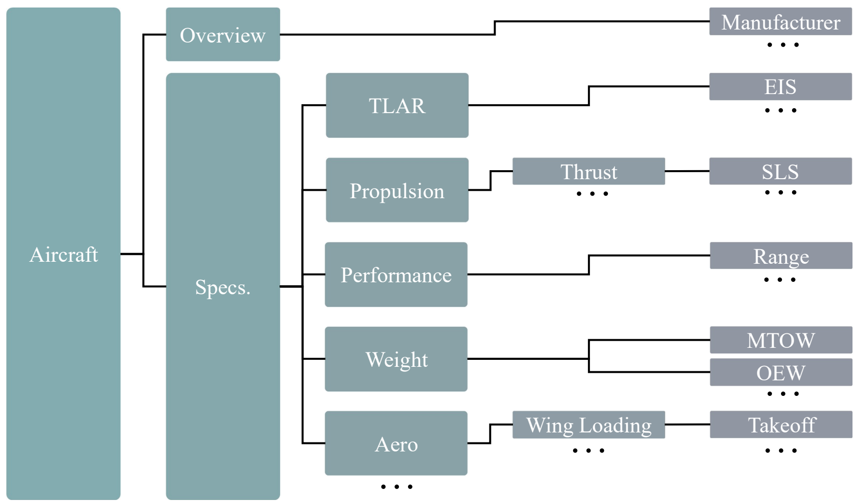

Fig. 1 Data storage structure for aircraft within the FAST tool.

D. S-Curve Modeling of Aircraft Performance Evolution

The database was leveraged to analyze the KPPs that represent the structural, aerodynamic, and propulsion efficiency over the years. These KPPs were examined in relation to both entry-into-service dates of the aircraft and other performance parameters, with the aircraft categorized by aisle type to yield more pronounced trends.

To investigate the historical evolution of KPPs and their connection with other aircraft specifications, scatter plots were used for visual analysis. By superimposing regressions (generally linear) over the scatter plots, general trends of the parameters through time and relationships between parameters can be investigated. Figures include the coefficient of determination, R^2, which is a statistical measure indicating how much of the variation in the dependent variable is explained by the independent variable. R^2 values range from 0 to 1, where values close to 0 suggest that the model does not explain much of the variability in the outcome, while values close to 1 indicate that a large proportion of the variance in the dependent variable is explained by the model. As mentioned earlier, regressions are used primarily to observe general trends, as opposed to predictive modeling, so R^2 values are not expected to be very high. In addition to regression lines, bivariate normal density ellipses are superimposed over the scatter plots, and correlations between the relevant parameters are observed visually. The bivariate normal density ellipse is the graphical representation of the bivariate normal density function [25]. Ellipses are drawn with a 90% confidence level, meaning there is a 90% chance that data from the distribution will fall within the ellipse. The orientation of this ellipse allows for understanding the strength and direction of the relationship between the parameters. For example, a circular ellipse indicates that there is no strong correlation between the data, whereas more elongated ellipses show that there is a strong correlation between the data. Moreover, the correlation coefficient (Eq. 2), which indicates the strength and direction of the linear relationship between two variables, is calculated and displayed in the graph. The coefficient ranges from -1 (a perfect negative relationship) to 1 (a perfect positive relationship). Bivariate normal density ellipse were obtained from JMP [26].

$$r = \frac{\text{cov}(X, Y)}{\sigma_X \sigma_Y} \tag{2}$$

where:

- $\text{cov}(X, Y)$ is the covariance between the two variables X and Y,
- σ_X is the standard deviation of X,
- σ_Y is the standard deviation of Y.

During the examined historical evaluation, TSFC has shown a direct correlation with technological advancement in engine technology. The remaining KPPs (OEW/MTOW, T/W, L/D) do not evolve directly with technological development. Instead, they are more related to performance requirements and the type of aircraft. Therefore, even if direct technological improvements exist, they may not be evident in the historical evaluation.

To model the evolution of technology that demonstrate a direct correlation with technological advancements, the Boltzmann Sigmoid, or S-curve, methodology was utilized. S-curves are characterized by four key parameters: the upper asymptote (U), indicative of the maximum achievable performance; the lower asymptote (La), representing the baseline performance; the inflection point (τ), where the rate of advancement transitions; and the growth rate (k), reflecting the pace of technological improvement. These parameters collectively delineate the progression from gradual improvements to rapid advancements and ultimately, the deceleration of gains as technologies reach maturity. To accurately determine the asymptotes of these S-curves, an investigation was conducted into the physical phenomena that could present barriers to technological advancement. These barriers include both inherent physical limitations and operational constraints, shaped by design requirements and regulatory standards. This approach ensures that the S-curves accurately reflect the theoretical and practical ceilings for technology advancement. Subsequently, historical data was fitted to these S-curves, with the quality of fit assessed using the coefficient of determination (R^2). During the fitting process, the lower and upper asymptotes were determined based on physical considerations based on physical considerations which are discussed for each S-curve further in detail in Section III.C. The inflection point was selected based on the rapid improvement observed. Quasi-Newton optimization algorithms were applied to select the growth rate, enhancing the fit (the R^2 value) between the S-curve and the historical data on KPPs. The resulting S-curves and the considerations that went into each curve is discussed in detail in Section III.

The S-curve equation, as given in Equation (3), utilizes the year of each data point (t) to model the progression of technological development. S-curves reflect the initial phase of gradual improvement, a rapid advancement toward the inflection point, and the final phase of slow performance improvements due to technology maturation. These phases can be seen in Figure 2. Notably, technology development can undergo significant breakthroughs, necessitating the development of new S-curves for the metrics of interest.

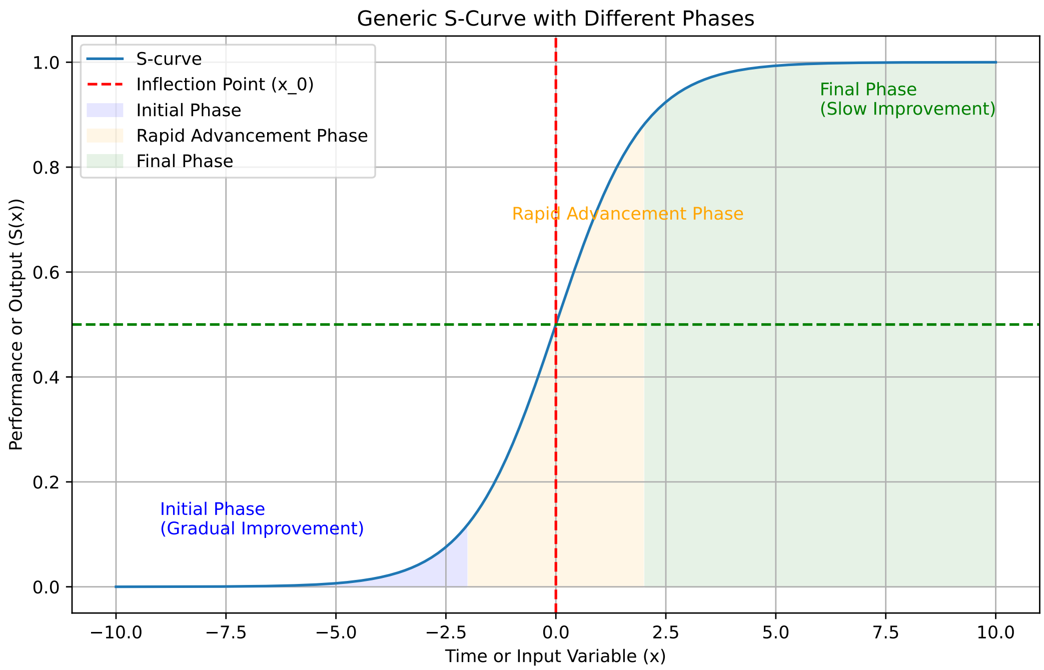

Fig. 2 Generic S-curve illustrating different phases of technological progression, including initial growth, rapid advancement, and maturation.

$$S(t) = La + \frac{U - La}{1 + e^{-k*(t-\tau)}} \tag{3}$$

For non-technological projections, estimates were made based on the continuation of historical trends after understanding the physical drivers behind them.

III. Examining Historical Trends and Future Projection

This section presents a historical evaluation of selected parameters (OEW/MTOW, T/W, TSFC, L/D) and future projections based on these trends. As described in Section II.B, data was collected from authorized sources, though certain aircraft were excluded from the analysis due to incomplete parameter information. Consequently, not all analyses include the same set of aircraft.

A. Operating-Empty-Weight-to-Maximum-Takeoff-Weight ratio (OEW/MTOW)

Aircraft design typically begins with weight estimations. For a given set of requirements, designers must estimate the payload weight ($W_{Payload}$) empty weight (W_{Empty}), fuel weight (W_{Fuel}), and maximum takeoff weight (MTOW, or W_0). This process generally involves calculating weight fractions. Equation 4 illustrates the relationship among the operational empty weight fraction (W_{Empty}/W_0, also denoted as OEW/MTOW), payload fraction ($W_{Payload}/W_0$), and fuel fraction (W_{Fuel}/W_0) [1].

$$\frac{W_{\text{Empty}}}{W_0} + \frac{W_{\text{Payload}}}{W_0} + \frac{W_{\text{Fuel}}}{W_0} = 1 \tag{4}$$

The fuel fraction mainly depends on mission requirements and performance characteristics, while payload weight is typically specified or inferred from design requirements. The operational empty weight relates to the aircraft configuration and type, and is often regarded as an indicator of structural efficiency, reflecting how effectively an aircraft's structure is designed relative to its total weight capacity [9]. However, interpreting trends in OEW/MTOW requires careful consideration, as this ratio is influenced not only by technological advancements (e.g., improvements in material science or structural optimization) but also by market-driven factors such as design range, aircraft size, and payload capacity.

An example of this influence is shown in Figure 3, which illustrates the relationship between aircraft range and OEW/MTOW. As range increases, OEW/MTOW tends to decrease because the aircraft must carry more fuel to cover longer distances. Additionally, not all components contributing to OEW (such as landing gear, control systems, and electronic systems) scale proportionally with MTOW [27]. Consequently, larger aircraft generally have lower OEW/MTOW ratios, which is sometimes interpreted as a sign of higher structural efficiency. However, the trends discussed in the following paragraphs suggest that this decrease in OEW/MTOW cannot be directly attributed to improvements in structural efficiency alone.

1. Study Design

The historical evolution of aircraft MTOW, size, range, and engine technology provides crucial insights into the drivers behind OEW/MTOW trends. To add more granularity, the aircraft in the database were categorized as either double-aisle or single-aisle. The general trends shown in Figure 4 suggest that OEW/MTOW has increased for single-aisle aircraft, with most data points concentrated between 0.5 and 0.6, while double-aisle aircraft show a slight decrease over time.

The data was also color-coded based on range, classified as short (under 1500 nm), medium (1500–4000 nm), and long (over 4000 nm). Aircraft with missing range data are marked as 'MS' (green points). Figure 4 reveals that certain range groups deviate from the general OEW/MTOW trends. For instance, the trends for long-range double-aisle aircraft

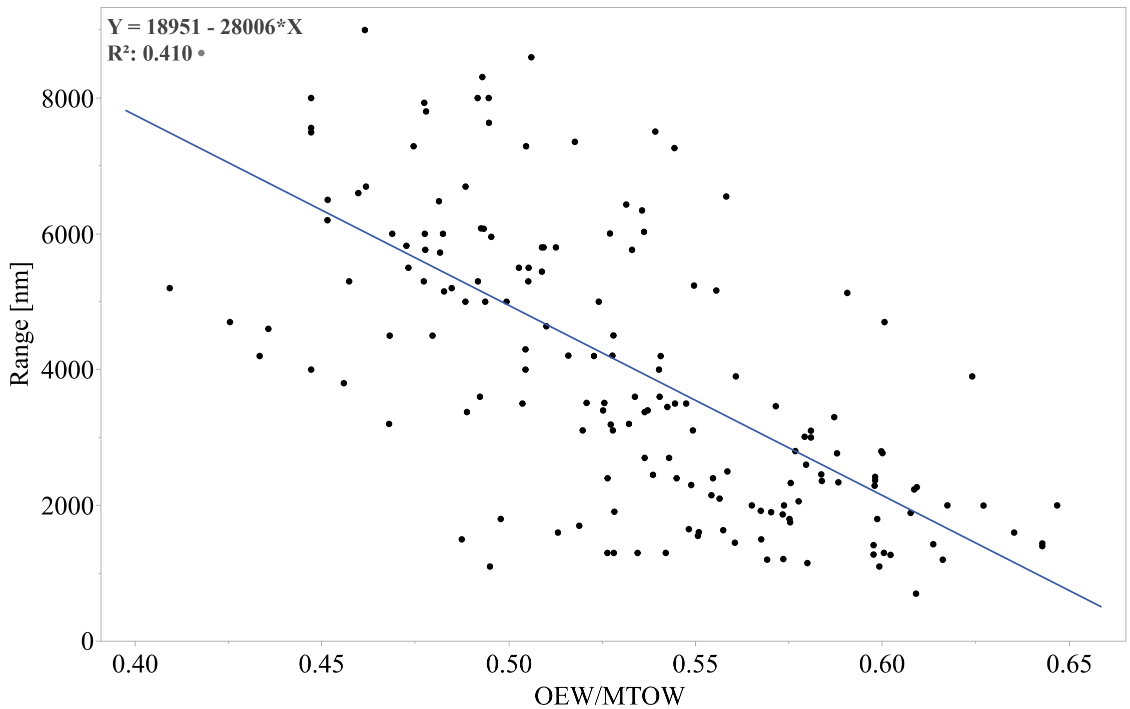

Fig. 3 Relationship between aircraft range and OEW/MTOW.

appear to be insensitive to the aircraft certification date, suggesting the need for a more detailed analysis of the impact of range and other factors.

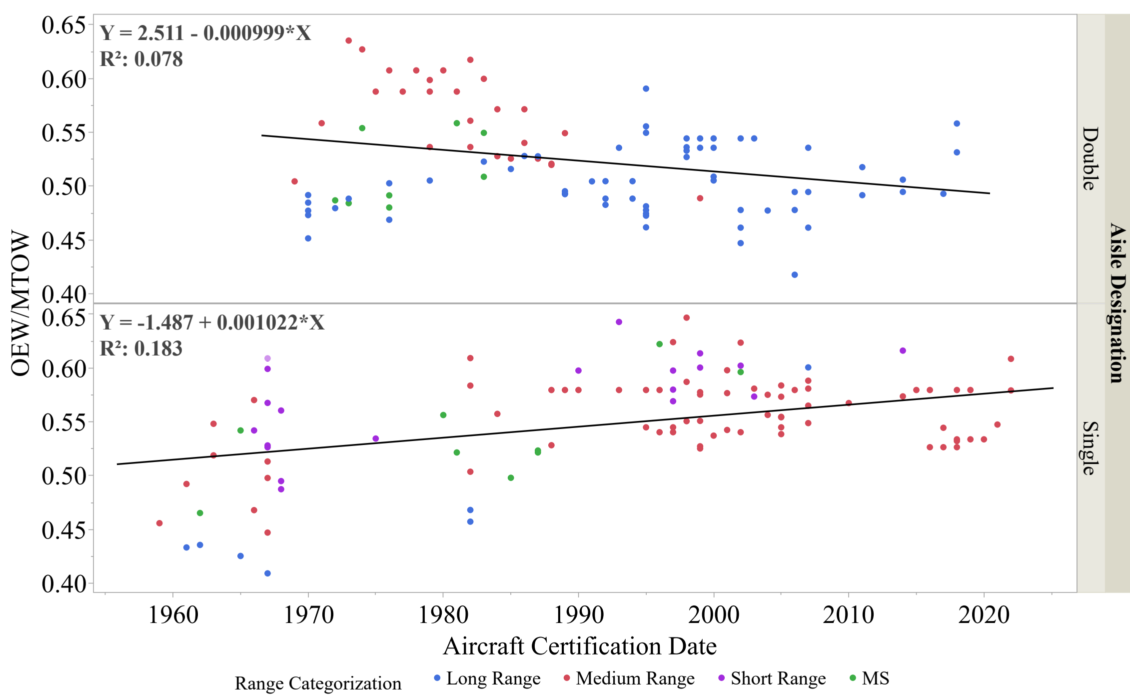

Fig. 4 Historical trends of OEW/MTOW for single-aisle and double-aisle aircraft over time, color-coded by range classifications.

It should be noted that in Figure 4, the OEW/MTOW ratios of some single-aisle aircraft produced between 1960 and 1970 were generally below the overall trend. These aircraft typically had four engines and were designed for medium- to long-range capabilities. Due to the lower efficiency of engines during that period, these aircraft carried more fuel, resulting in lower OEW/MTOW ratios. For double-aisle aircraft, models produced between 1970 and 1990 were often medium-range, leading to higher OEW/MTOW values. Later, medium-range aircraft began to be produced as single-aisle models.

2. Impact of Range, Size, and MTOW

Figure 5 shows that the range of double-aisle aircraft has gradually increased, reflecting design choices favoring long-haul capability. However, there is no clear trend of range growth for single-aisle aircraft, as indicated by the low R^2 value. This suggests that designs in this category prioritize cost-efficiency and short-haul performance rather than extending range.

Similarly, Figure 6 indicates an increase in the size of double-aisle aircraft over time, with Figure 7 showing a corresponding rise in MTOW. In contrast, the size and MTOW of single-aisle aircraft do not exhibit consistent growth, reflecting their role in short- to medium-range operations where flexibility and economic considerations are prioritized over size increases.

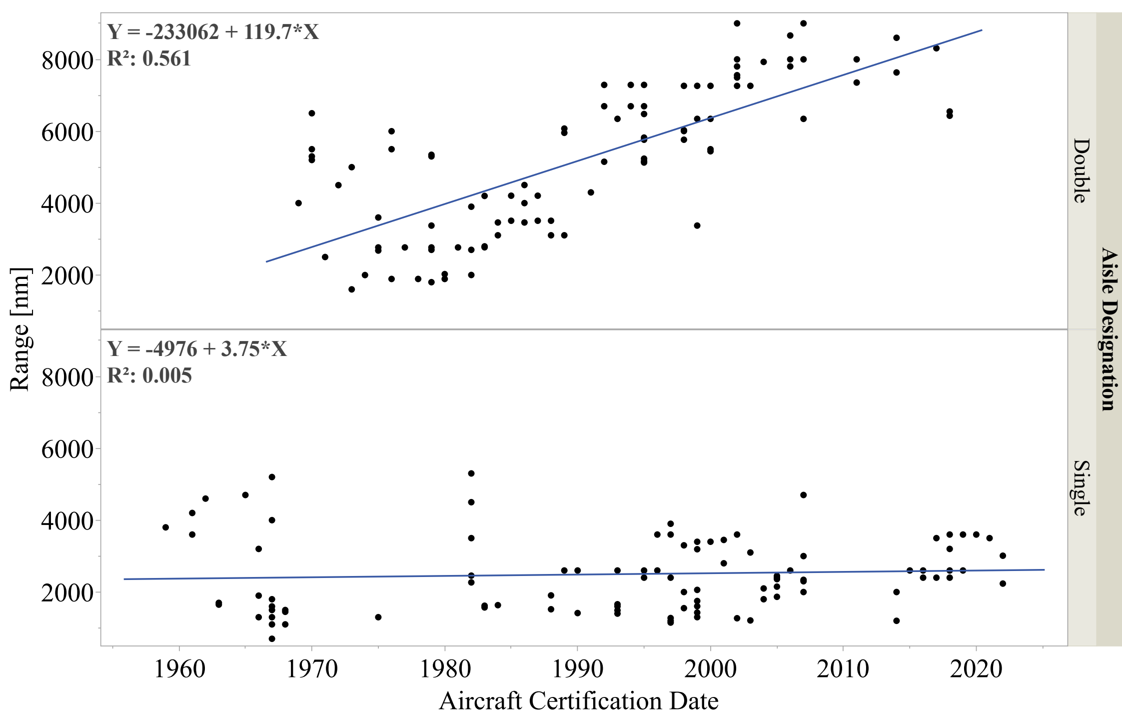

Fig. 5 Evolution of aircraft range over the years for single-aisle and double-aisle configurations, demonstrating differences in range trends.

As a result, the decrease in OEW/MTOW for double-aisle aircraft does not necessarily indicate improvements in

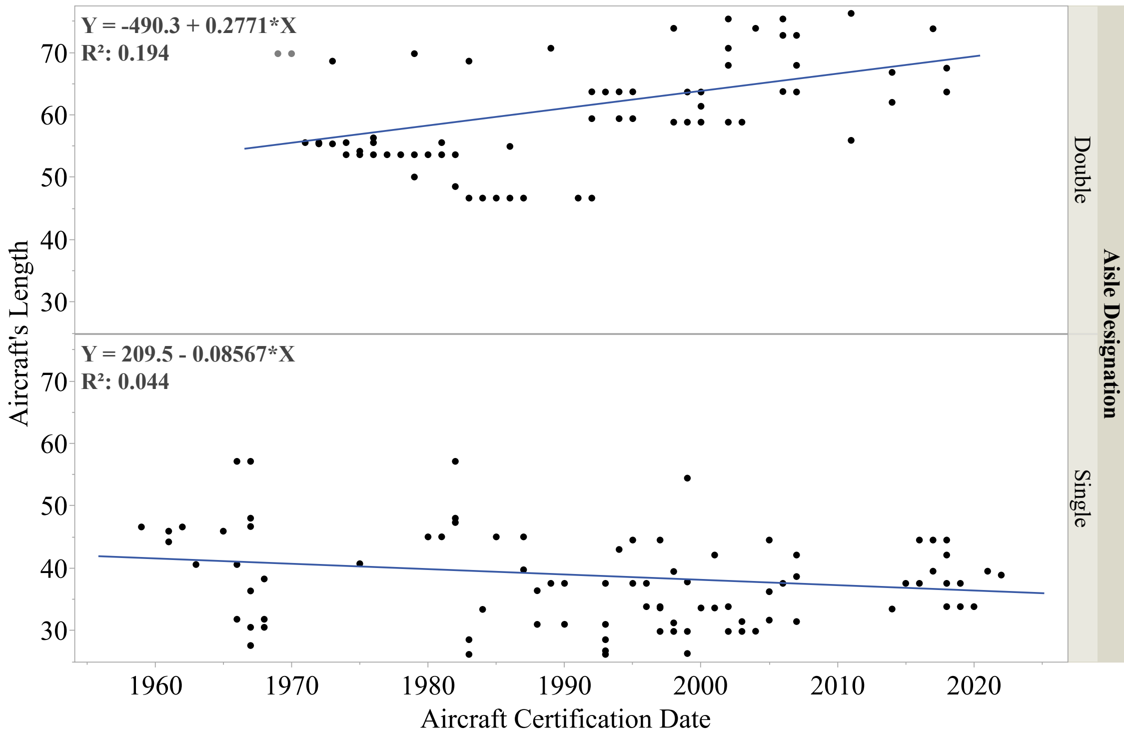

Fig. 6 Change in aircraft length over time for single-aisle and double-aisle aircraft.

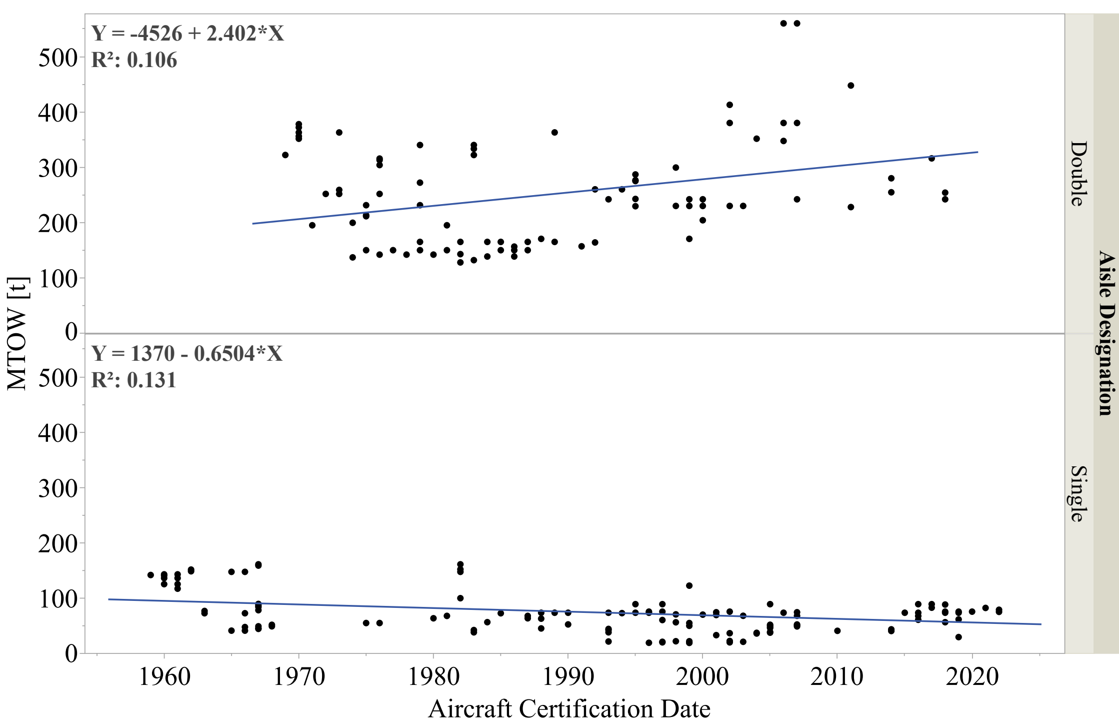

Fig. 7 Maximum takeoff weight trends for single-aisle and double-aisle aircraft over the years.

material technology. Instead, this reduction is more closely correlated with increased range and aircraft size, as data shows that double-aisle aircraft have achieved greater range and weight capabilities over time.

3. Influence of Engine Weight

Figure 8 reveals that the engine weight fraction for double-aisle aircraft has decreased over the years, while it has slightly increased for single-aisle aircraft, despite no consistent rise in MTOW (as seen in Figure 7). Engine weight is part of the operating empty weight, and these trends align with the OEW/MTOW patterns observed in Figure 4. This suggests that changes in engine weight fraction also likely contribute to the overall OEW/MTOW trends. Thus, the rising trend in OEW/MTOW for single-aisle aircraft is potentially impacted by the higher engine weight fraction.

4. Other Factors

Improvements in passenger comfort, such as the incorporation of heavier seats and entertainment systems, along with technological advancements for safety and reliability, may lead to an increase in OEW/MTOW. However, these factors are challenging to quantify directly [9, 28].

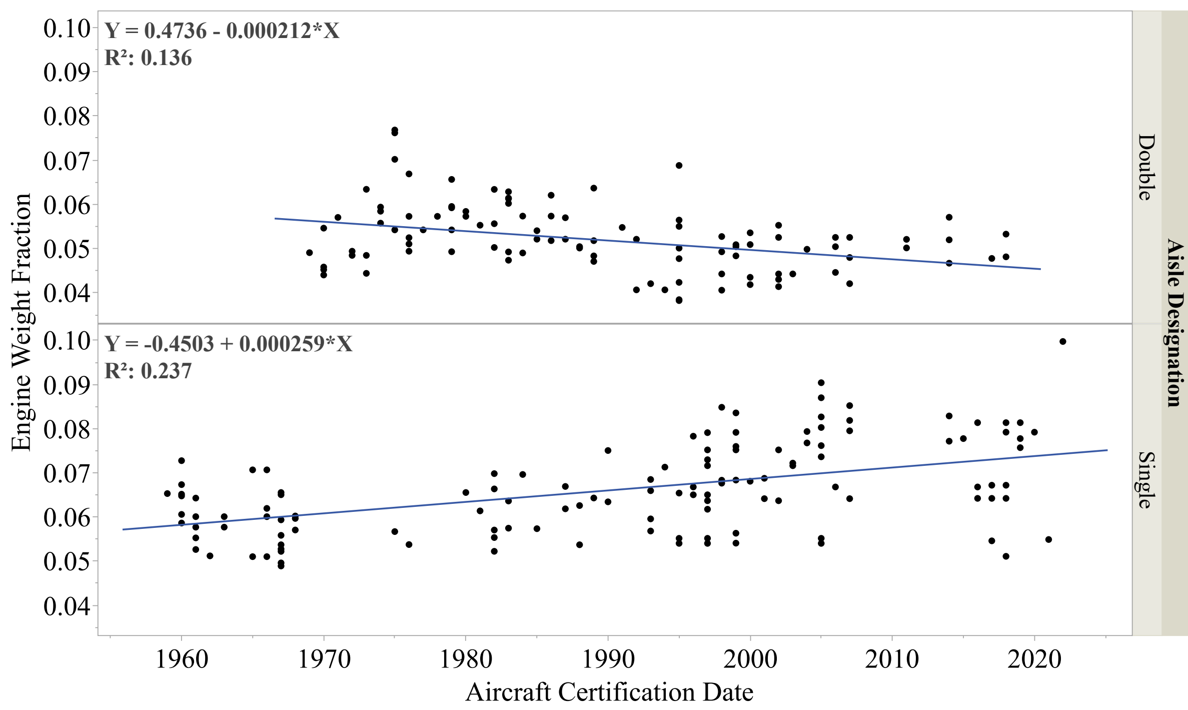

Fig. 8 Trends in engine weight fraction over time, grouped by single-aisle and double-aisle aircraft.

5. Material Technology and Structural Efficiency: A Case Study

The analyses thus far show that it is rather challenging to directly attribute changes in this ratio to material advancements, such as composites and lightweight aluminum, solely based on the historical trends of OEW/MTOW.

Even where these materials have been adopted, their effects may not be immediately evident from broad historical analyses. However, this does not imply that material improvements have no influence on empty weight fraction. To accurately assess the impact of lightweight materials on OEW/MTOW, a direct comparison of aircraft with similar top-level design requirements, such as passenger capacity and range, would be necessary.

To explore this hypothesis, two aircraft with similar design requirements are compared in Table 1. The top-level design parameters of the A330-900, certified in 2018, and the A350-900, certified in 2014, are fairly similar. For instance, the A330-900 has a passenger capacity of 310 and a range of up to 7,200 nm, while the A350-900 can carry 315 passengers and fly up to 8,300 nm. Their overall dimensions are also similar. The A350-900 is primarily constructed using composite materials, whereas the A330-900 is mostly made of aluminum [29]. Comparing the OEW/MTOW ratios, the A350-900 has a 10% lower operational empty weight fraction. Given that the design and performance parameters of these two aircraft are very similar, this lower OEW/MTOW is likely attributable to the use of composite materials in the A350-900.

Table 1 Comparison of A330-900 and A350-900 [11].

	Length [m]	Wingspan[m]	Range nm	Passenger (2-Class)	OEW/MTOW
A330-900	63.66	64	7200	310	0.559
A350-900	66.80	64.75	8300	315	0.506

6. Fuel Fraction Trends and Cost Efficiency

When examining the changes in fuel fraction over the years (Figure 10), it is clear that the fuel fraction for double-aisle aircraft has not increased at the same rate as their range (Figure 5), implying improvements in fuel efficiency. However, the low R^2 value for double-aisle aircraft fuel fraction trends indicates a weak correlation, implying that while the general trend points to efficiency gains, there are other factors (such as engine or aerodynamic improvements) influencing fuel consumption. Conversely, the range trends for single-aisle aircraft have remained relatively stable (Figure 5), as has their payload capacity (Figure 9), yet a significant reduction in fuel fraction is observed. This pattern, coupled with a weak correlation in R^2 for range and fuel, indicates that other factors have led to fuel savings even without extending range capabilities. These improvements align with broader trends towards operational efficiency in the single-aisle segment, where maintaining low operational costs per passenger per unit of range is a key objective.

Figure 11 illustrates changes in this cost metric over the years for both double-aisle and single-aisle aircraft, showing a consistent decline. The stronger R^2 values suggest that these reductions have been a significant and reliable trend, driven by advances in propulsion, aerodynamic refinements, and weight optimization. While fuel efficiency has been a major factor in reducing costs, improvements in structural efficiency (as seen in OEW/MTOW) are less evident in broad historical evaluations.

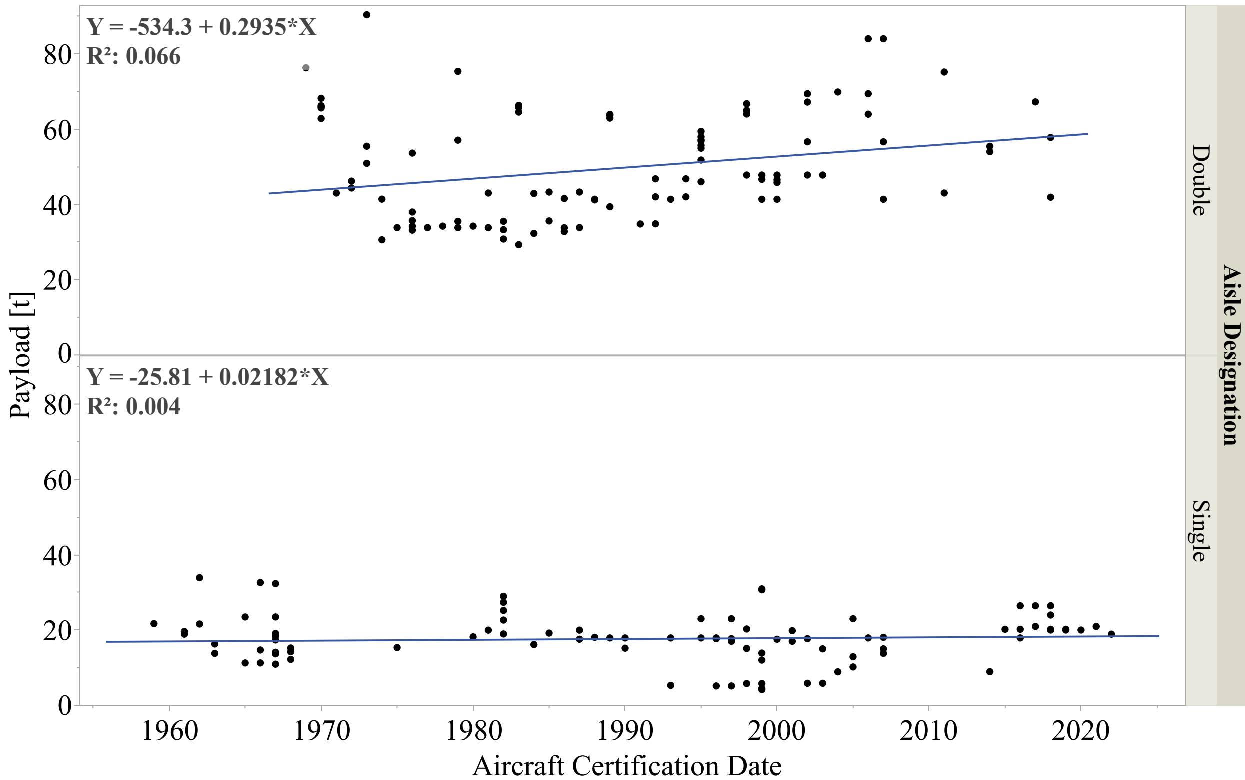

Fig. 9 Historical payload capacity trends for single-aisle and double-aisle aircraft.

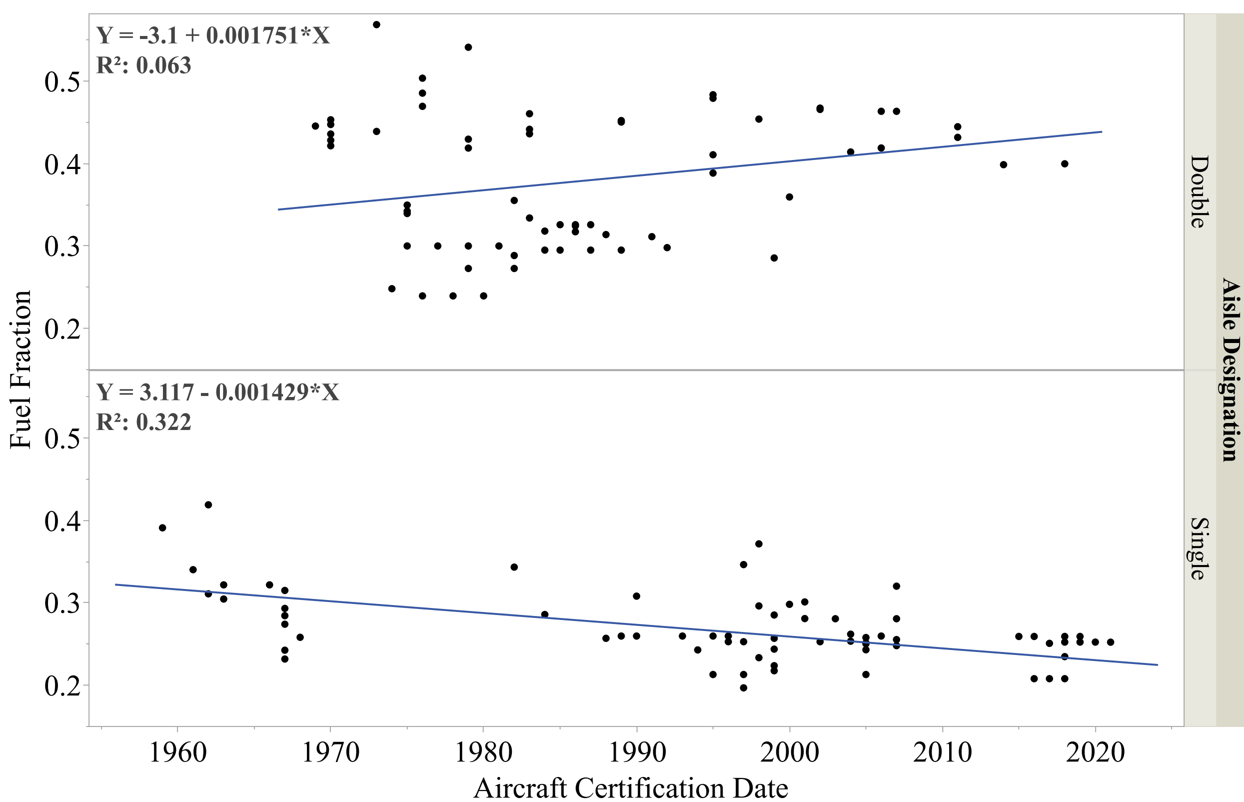

Fig. 10 Evolution of fuel fraction over time for single-aisle and double-aisle aircraft.

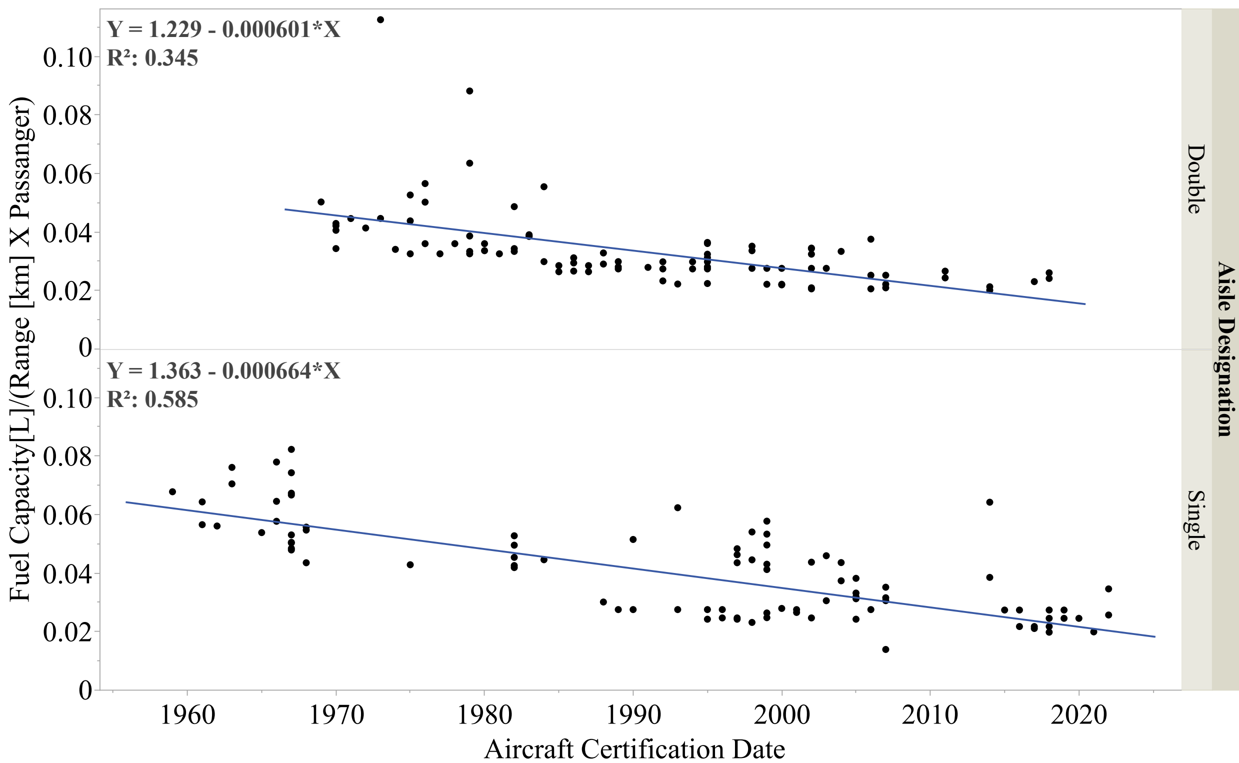

Fig. 11 Trends in fuel efficiency measured as fuel capacity per range per passenger for single-aisle and double-aisle aircraft, showing the reduction over time.

7. Summary of OEW/MTOW Trends

To sum up, OEW/MTOW trends do not directly indicate structural efficiency. Evaluations must consider top-level requirements, such as range and size, when comparing aircraft structural efficiencies.

For future estimates, market demand is assumed to remain relatively stable, with aircraft size, MTOW, and range expected to stay the same. Additionally, no radical changes in propulsion technology are anticipated. Excluding outlier aircraft, the average OEW/MTOW ratio is 0.56 for single-aisle and 0.51 for double-aisle aircraft.

B. Thrust-to-Weight ratio (T/W)

The thrust-to-weight ratio (T/W), defined as the ratio of sea-level static thrust to maximum takeoff weight of the aircraft, is a crucial parameter influencing aircraft performance and is closely related to the wing loading (W/S), the ratio of MTOW to the aircraft's wing area [1, 30].

Analyzing the relationship between the four main forces acting on an aircraft, namely thrust, drag, lift, and weight, yields a functional connection between T/W and W/S. Mattingly represents this relationship in Equation 5, referred to as the "constraint master equation" [30]. This equation establishes constraint boundaries for T/W and W/S, derived from both aircraft design requirement and regulatory constraints, such as cruise speed, turn rate, climb rate, approach speed and takeoff field length. Figure 12 illustrates a sample constraint diagram, with W/S on the horizontal axis and

T/W on the vertical axis. Once all constraints are defined, the objective is to minimize the T/W ratio and select the optimal point in the solution space. Both T/W and W/S are typically selected early in the design phase [30].

$$\frac{T}{W} = \frac{\beta}{\alpha}\left(\frac{qS}{\beta W}\left[K_1\left(\frac{n\beta}{q}\frac{W}{S}\right)^2 + K_2\left(\frac{n\beta}{q}\frac{W}{S}\right) + C_{D0} + C_{DR}\right] + \frac{P_s}{V}\right) \tag{5}$$

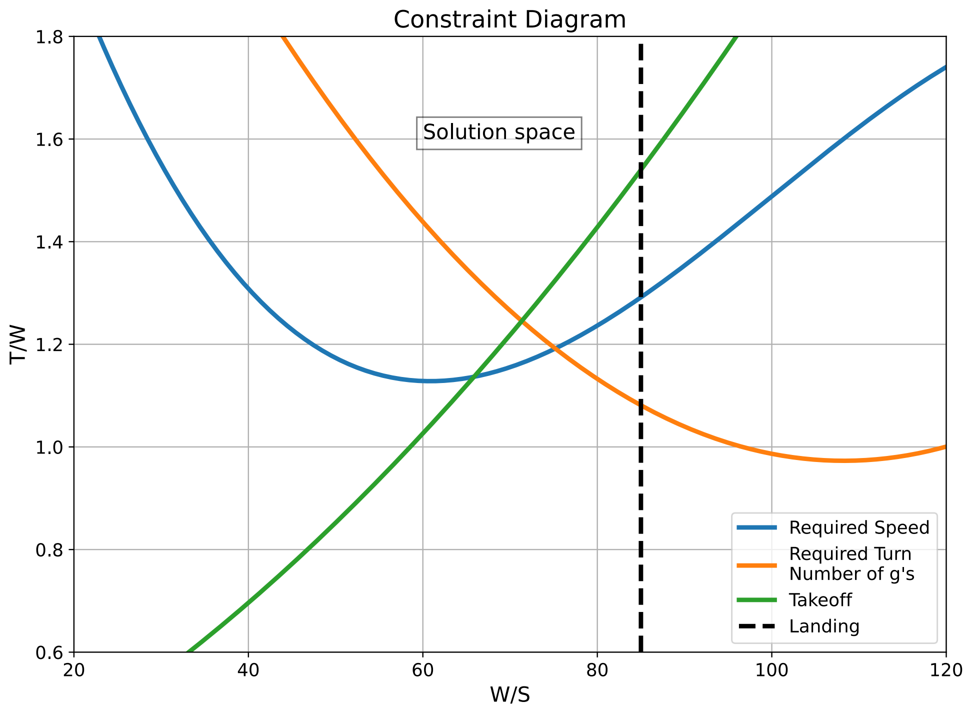

Fig. 12 Notional constraint diagram illustrating thrust-to-weight (T/W) ratio versus wing loading (W/S), based on performance constraints. Recreated from [30].

When investigating T/W over the years in Figure 13, values range from 0.21 (corresponding to the DC-8-31) and 0.42 (corresponding to the CRJ550). The T/W ratio generally increased around the 2000s and has since remained stable. To understand the reasons behind these trends, aircraft were categorized by aisle configuration, as shown in Figure 14. Observing the thrust-to-weight (T/W) ratio trends for both double-aisle and single-aisle aircraft, it can be seen that the T/W ratio is increasing for single-aisle aircraft, while it is slightly decreasing for double-aisle aircraft. The relationship of these trends with engine thrust and MTOW is explained in Section III.B.1. In addition, in Equation 5, the term β is defined as the ratio of the instantaneous weight W to the takeoff weight W_{TO}, represented as $\beta = \frac{W}{W_{\mathrm{TO}}}$ [30]. This term depends on fuel efficiency and payload delivery. Fuel efficiency increases over time, as seen in the Figure 11, and this may play a role in the increase of the T/W ratio.

1. Influence of Maximum Engine Thrust and MTOW

Figure 15 shows the maximum takeoff thrust of engines from 1956 to 2020, categorized by aisle designation. Maximum thrust ratings for engines used in double-aisle aircraft have significantly increased over time, whereas only a slight increase is observed in the single-aisle category. In single-aisle aircraft, the increase in the T/W ratio, along with improved fuel efficiency, stems from a reduction in MTOW and an increase in thrust. For double-aisle aircraft, although engines with higher thrust were developed, the weight of the aircraft on which these engines are installed has also increased proportionally with thrust, resulting in no clear trend in T/W change. In the database, the most powerful engine is recoded as the GE9-115B, producing 513.9 kN, while the least powerful is the ALF502R-3A, producing 31 kN—over16 times less than the GE9-115B. However, this variation in thrust levels does not directly indicate changes in the T/W ratio, as T/W is highly influenced by design requirements, regulatory constraints, and weight, as discussed previously. Additionally, T/W is closely related to W/S, and not dependent solely on the engine technology.

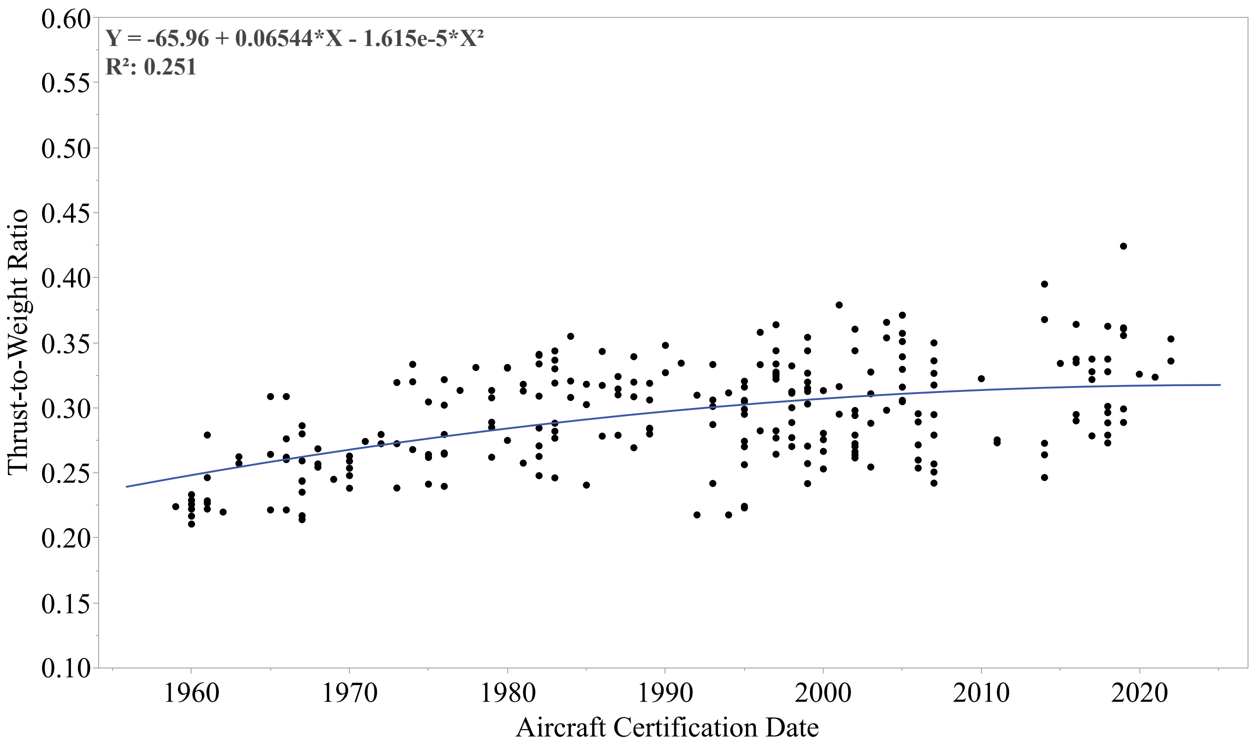

Fig. 13 Historical trends in thrust-to-weight ratio for aircraft.

2. Influence of Aircraft Type, Mission, and Performance Requirements

In the early design phase, Raymer [1] categorizes T/W based on intended aircraft use, such as military, fighter, or transport applications. The categorization further divides fighter aircraft into subcategories like trainers and dogfighters, emphasizing that T/W directly reflects mission-specific performance parameters.

An example on the impact of performance requirements on T/W is the takeoff field length and its effect on T/W

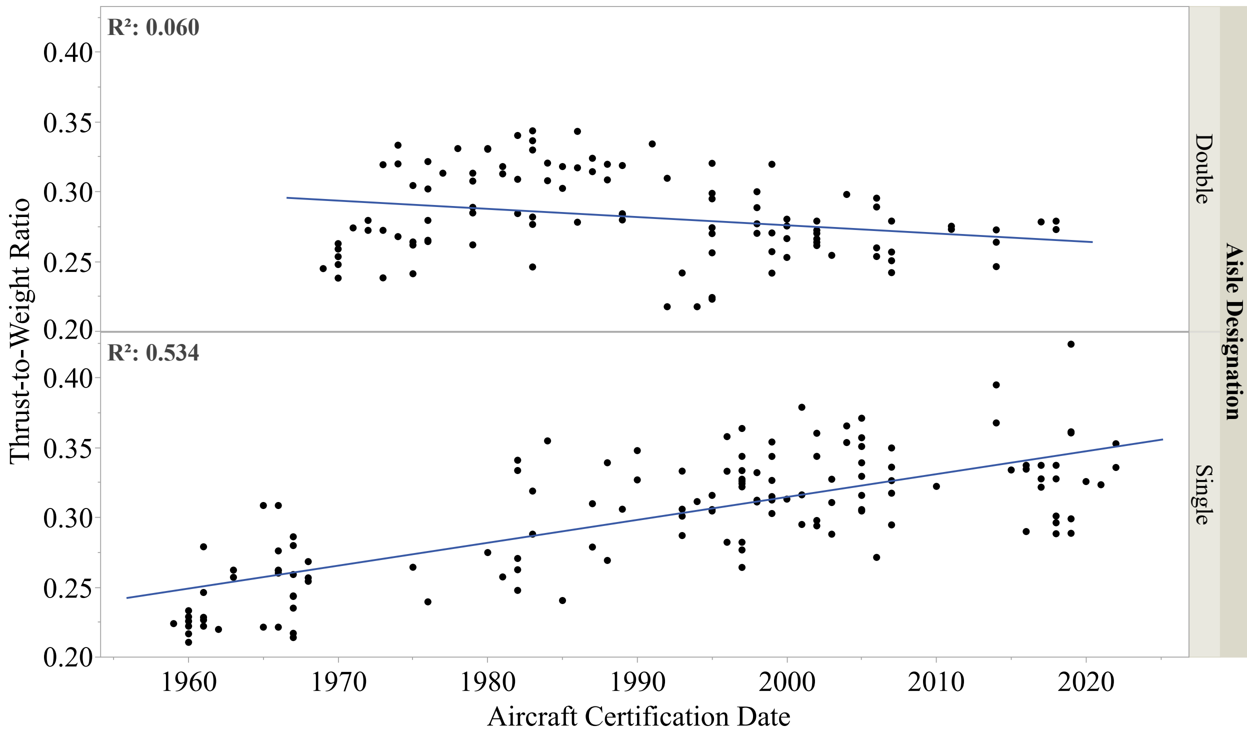

Fig. 14 Historical trends in thrust-to-weight ratio for aircraft by aircraft aisle designation.

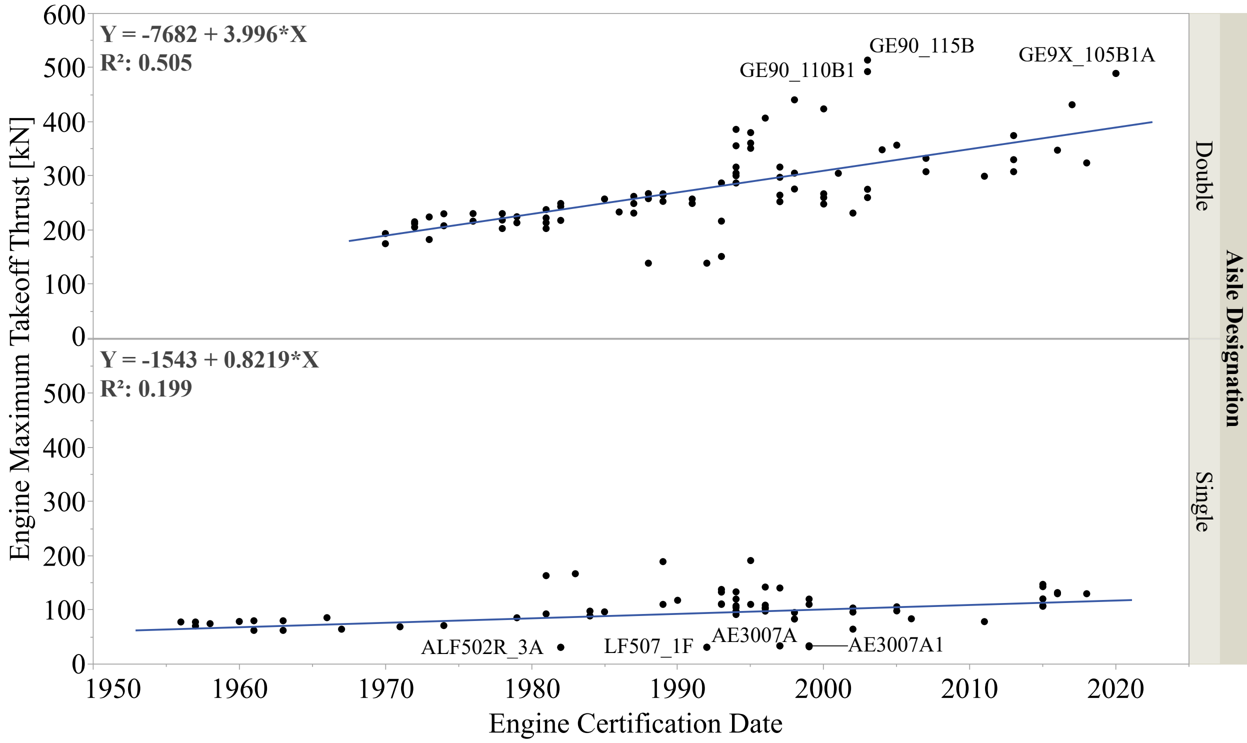

Fig. 15 Maximum takeoff thrust of engines over time, color-coded by aircraft aisle designation, illustrating the evolution of engine performance.

requirements, as shown in Figure 16. Aircraft with lower T/W ratios require longer takeoff distances because T/W directly affects acceleration, meaning a longer runway is needed to reach takeoff speed—impacting airport compatibility and operational requirements. Alternatively, this trend can also be viewed from the perspective that aircraft designed to operate from longer runways can opt for less powerful engines, potentially reducing costs and saving weight. Both interpretations imply that knowing the required takeoff field length early in the design process enables optimization of T/W for specific field length constraints.

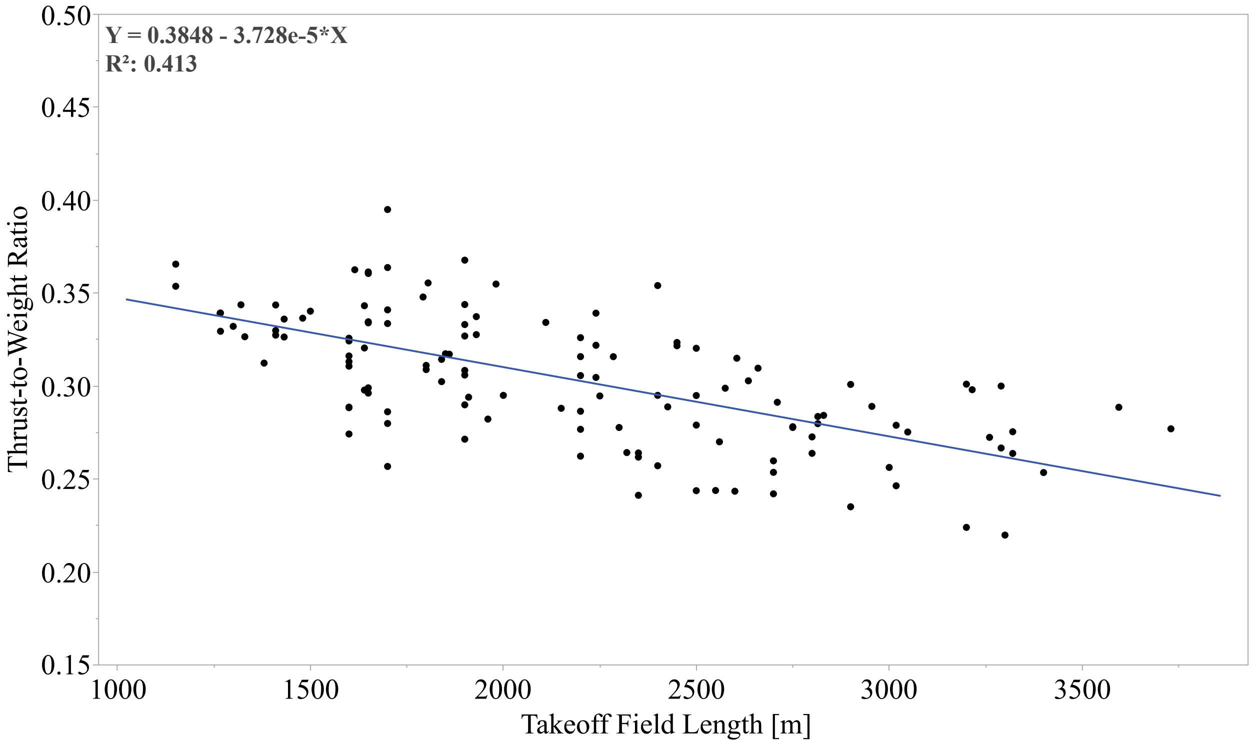

Fig. 16 Relationship between thrust-to-weight ratio and takeoff field length, demonstrating performance trade-offs.

3. Future Trends and Technological Constraints

In conclusion, T/W ratio depends on the aircraft type, fuel efficiency, and performance requirements. In this section, only subsonic commercial aircraft are considered, which is why there data is limited in its range. Furthermore, alteration of the performance requirements of the aircraft such as cruise speed, service ceiling, and turning rate of the aircraft are not substantial. Additionally, engine thrust is not anticipated to increase as significantly as in previous years. The reason for this is that thrust has a positive relationship with the bypass ratio. As the bypass ratio increases, thrust increases, and higher bypass ratio engines have a larger diameter. Relationship between engine's diameter and takeoff thrust can be observed from Figure 17. However, with the continuous advancement in engine technology, ground clearance limits will eventually be reached [31]. Therefore, T/W is not likely to undergo significant alterations in the future. if any changes occur, they may only lead to a slight increase. Based on this, no significant changes in the T/W ratio for commercial aircraft are expected in future years, as shown in Figure 18.

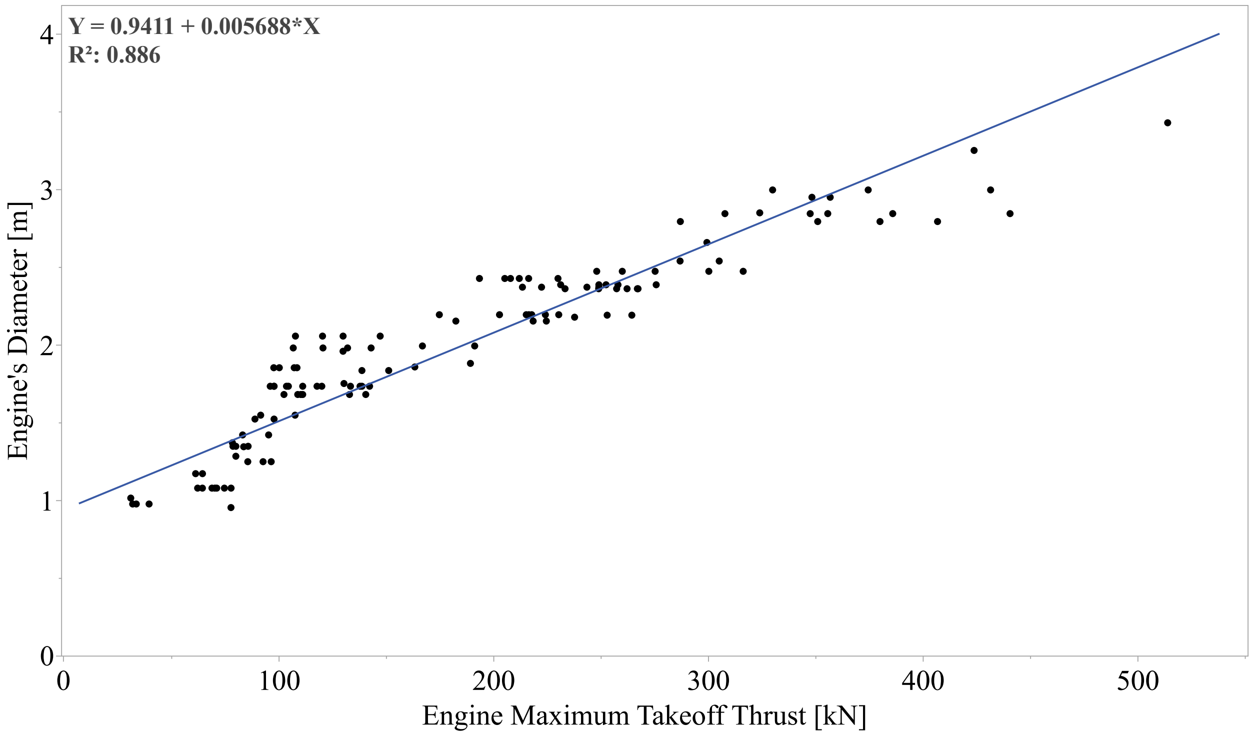

Fig. 17 Correlation between engine diameter and maximum takeoff thrust, highlighting engine design trends over time.

C. Thrust Specific Fuel Consumption (TSFC)

In aircraft design, fuel efficiency is a critical performance metric, with Thrust Specific Fuel Consumption (TSFC) serving as a measure of the fuel efficiency for turbofan engines [30]. TSFC is defined as the fuel consumption per unit time normalized by thrust, as defined in Equation 6 [32]. Lower cruise TSFC values reflect more efficient propulsion systems, and advancements in propulsion technology have led to notable TSFC reductions over time, as seen in Figure 19.

$$TSFC = \frac{\dot{m}_f}{T} \tag{6}$$

1. Factors Influencing TSFC Trends

While TSFC trends show a general decline with newer engine designs, several performance factors influence gas turbine efficiency. Studies from the National Academies of Sciences, Engineering, and Medicine (NASEM) in 2016 identified key engineering drivers in engine design: overall efficiency, weight, drag, and reliability [33]. Overall efficiency encompasses the efficiency with which the engine converts the chemical energy stored in fuel to propulsive

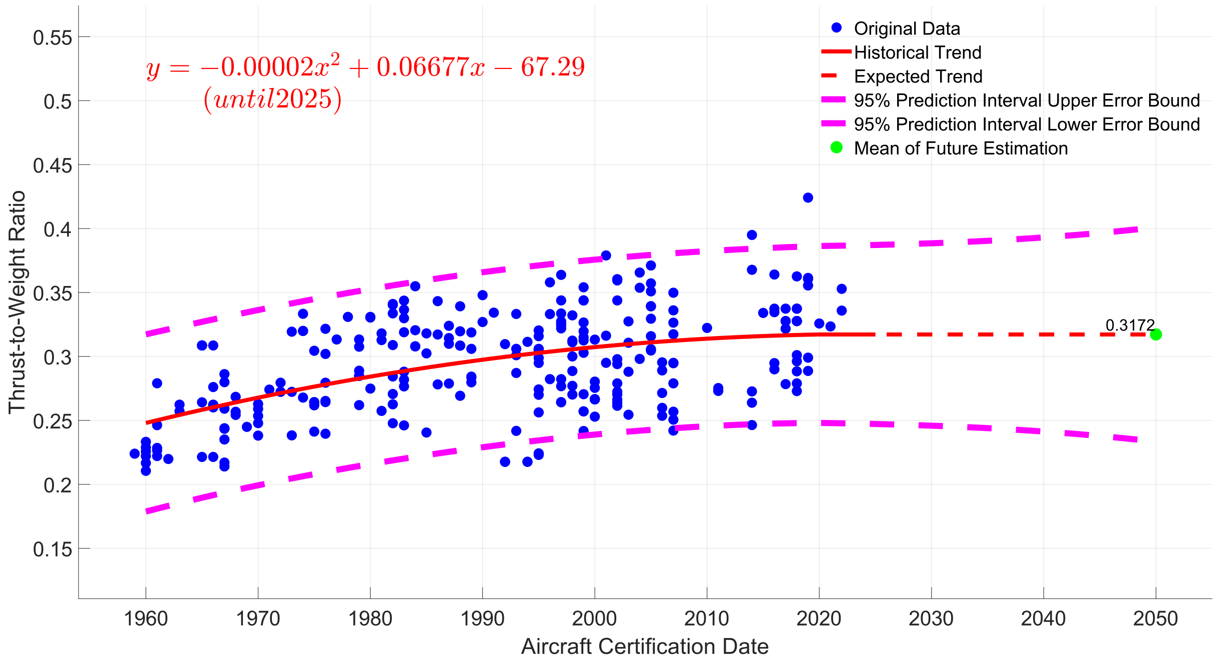

Fig. 18 Predicted changes in thrust-to-weight ratio over time for future commercial aircraft.

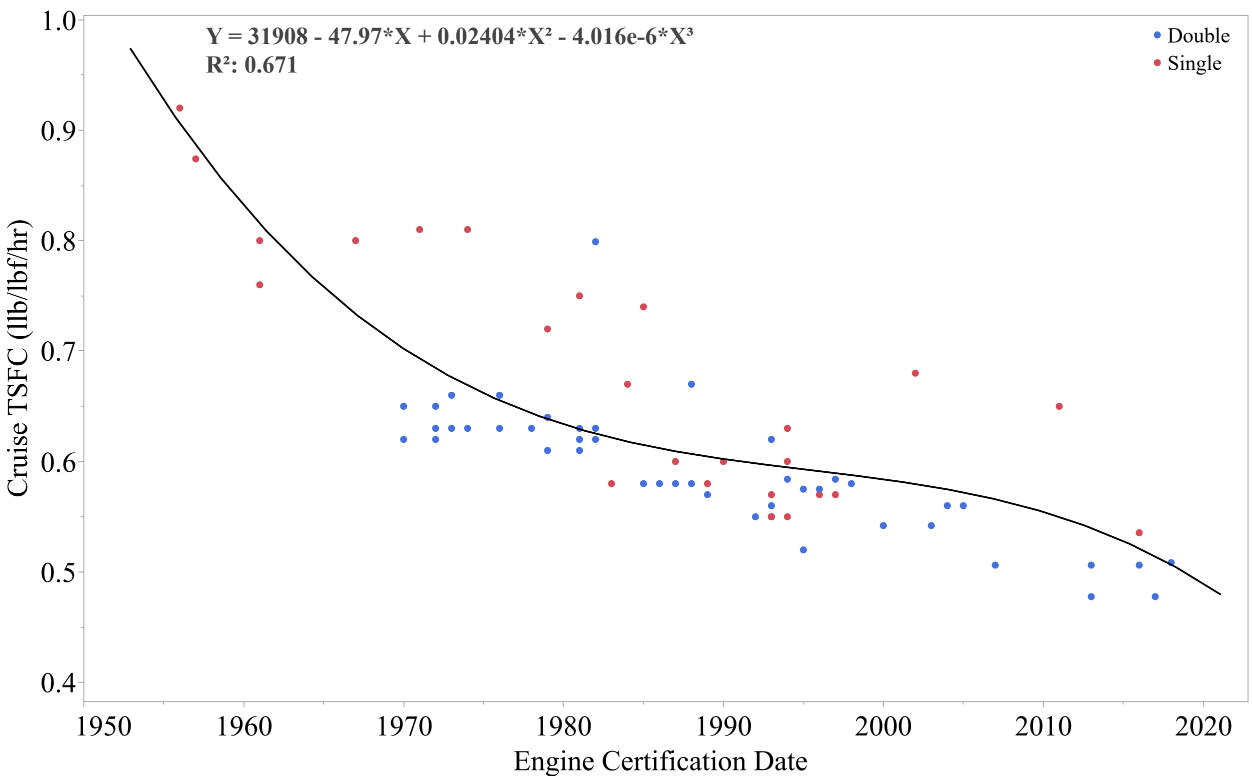

Fig. 19 Trends in thrust-specific fuel consumption relative to the engine certification year.

power. Current trends indicate that increases in propulsive efficiency demand larger engines, costing additional weight and drag. As such, committees in NASEM note that engines for long-range or double-aisle applications are optimized for higher efficiency levels due to the weight and cost studies for engine weight and fuel burn. Smaller or single-aisle aircraft favor smaller engines with cheaper cost of ownership and are not as efficient as ones used on double-aisle aircraft.

Figure 20 illustrates that TSFC decreases as engine diameter increases, reflecting efficiency gains from larger engine designs with high bypass ratios. In this study, TSFC is treated as a technological parameter, with future projections modeled using S-curves to account for expected improvements over time. For these projections, lower asymptotes were defined, representing the practical lower limit of cruise TSFC attainable through advancements in propulsion technology.

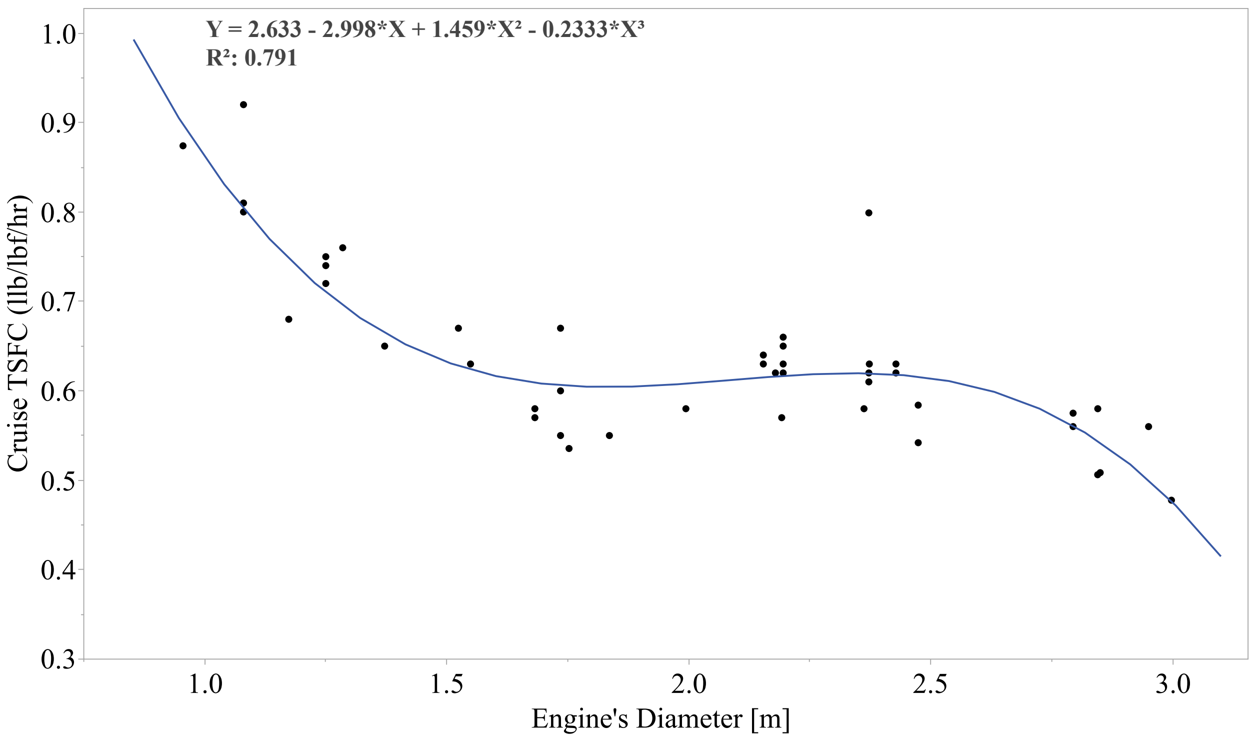

Fig. 20 Relationship between thrust-specific fuel consumption and engine diameter, indicating efficiency gains associated with larger engines.

Torenbeek's high-level TSFC expression in Equation (7) accounts for factors such as cruise Mach number M_o, cruise ambient to sea level temperature ratio θ, and overall engine efficiency η_{tot}, which combines combustion, propulsive, and thermal efficiencies. This equation highlights the physical determinants of TSFC, including maximum cruise altitude, air temperatures at cruise and sea level, and engine component efficiencies.

$$SFC = 0.2788 * \frac{M_o * \sqrt{\theta}}{\eta_{tot}} \tag{7}$$

The present scope of the study encompasses only subsonic transport aircraft, which limits the consideration of cruise Mach number to less than unity. Based on the historical maximum operating cruise Mach number data shown in Figure 21, turbofans typically cruise between Mach 0.7 and 0.95.

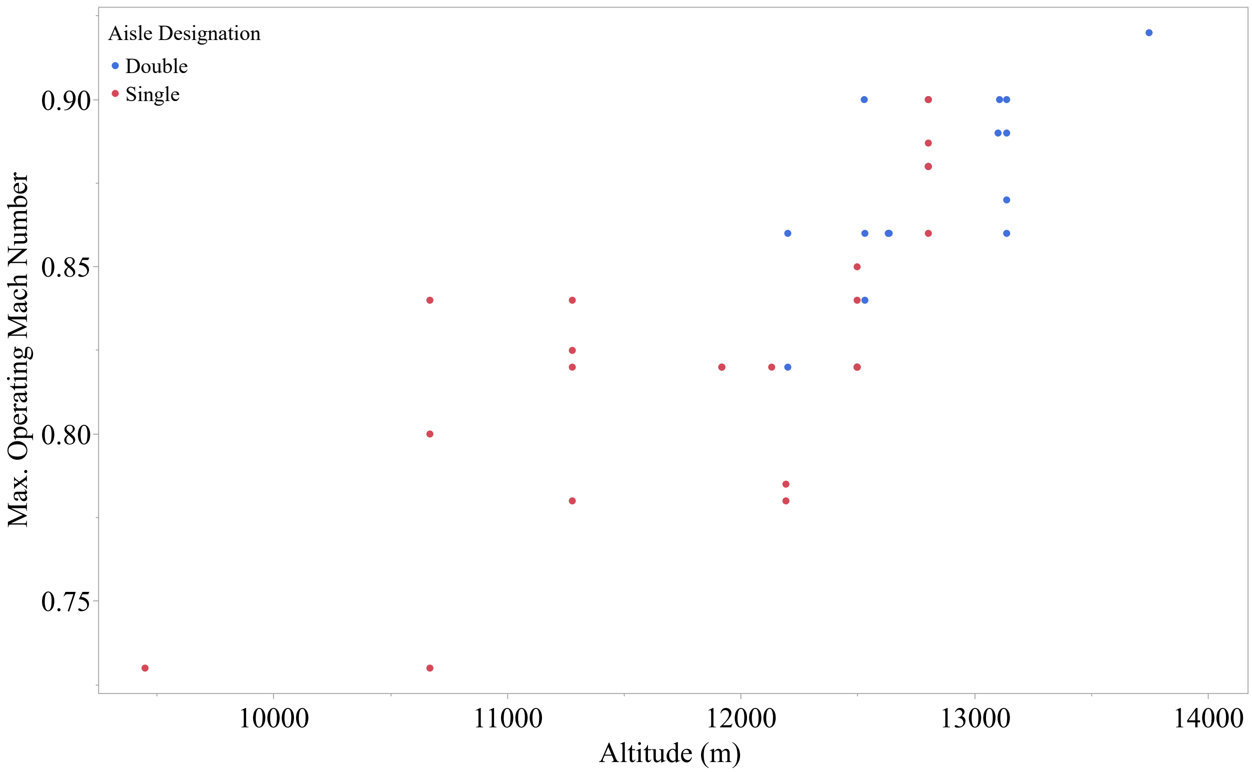

Fig. 21 Maximum operating Mach number versus cruise altitude for single-aisle (red) and double-aisle (blue) aircraft.

It was noted in data collection that TCDSs often record only the maximum operating cruise Mach number instead of the typical cruise Mach number, as the latter can vary depending on the flight mission profile. However, a limited number of aircraft manufacturer's Airport Planning Manuals (APM) payload-range diagrams, which document actual cruise Mach numbers. Analysis of these diagrams reveals that aircraft generally cruise at a lower Mach number than the maximum operating limit. For example, while Boeing 757 and 767 both have a maximum operating cruise Mach number of 0.86, they typically cruise at Mach 0.8. This cruise Mach number of 0.8 was in fact found to be the mean of the recorded values and was used for verification and lower asymptotic value projection in this study.

The cruise ambient to sea level temperature ratio θ is driven by the maximum cruise altitud, which is generally optimized for efficiency under FAA altitude certification limits and the structural pressurization load limits of the fuselage. As shown in Figure 21, , the historical data indicates that aircraft in the databse operate at cruise altitudes ranging between 30,000 to 51,000 feet.

At these typical cruise altitudes, air temperature stabilizes around 392.67 °R. . When normalized against sea-level temperature of 518.07 °R, this yields a temperature ratio of $\theta = 0.75795$. Lastly, TSFC is also driven by the overall engine efficiency, which includes factors such as propulsive, combustion, and thermal efficiencies.

Achieving high levels of propulsive efficiency, such as those exceeding 0.8, is technically challenging and demands ongoing research into materials science, manufacturing, turbomachinery, heat exchangers, low-emission combustion systems, controls, and simulation capabilities. According to Singh et al. [34], a propulsive efficiency of higher than 0.8 can be reached with advanced turbofan engines and future technologies such as open-rotor (propfan) engines, as well as operating at lower cruise Mach numbers and using engines with higher bypass ratio.

As of 2012, the overall engine efficiency η_{tot} was estimated to be around 0.35, which remains well below the theoretical upper limit identified by Singh et al. [34]. The limitation on η_{tot} is primarily driven by the turbine entry temperature (TET), overall pressure ratio (OPR), and combustion that ensures low nitrogen oxide (NOx) emission. Assuming the combustion is with hydrocarbon fuel, the TET for low NOx emission is limited between 2000 and 2100 Kelvin. Under these conditions, the practical upper limit for η_{tot} is 0.55. With a cruising Mach number of 0.8, cruise altitude of 35,000 ft, and η_{tot} of 0.55, the practical limit for cruise TSFC is 0.353 lb/lbf/hr.

If environmental impact and material limits are ignored, the theoretical limit of η_{tot} could reach as high as 0.65. This would assume stoichiometric combustion (2600 K), ideal component efficiencies, and OPR higher than 80. With these conditions applied, the theoretical limit for TSFC at a cruise Mach of 0.8 and altitude of 35,000 feet is 0.299 lb/lbf/hr.

2. S-Curve Projections and Efficiency Limits

Figures 22a to 22c show the S-curve projections using the practical limit, theoretical limit, and NASA 2019 ARMD cruise TSFC as lower asymptotes. Specifications for these S-curve models, including asymptotic values, inflection points, growth rates, and corresponding R^2 values, are detailed in Table 2. Both the practical and theoretical limits were derived using the aforementioned cruise conditions, but with overall efficiencies of 0.55 and 0.65, respectively. The NASA 2019 ARMD projection reflects a conservative mid-term technology target, estimating a 50% improvement relative to the 2005 best-in-class engine. This engine is identified as the CFM56-7B used in the Boeing 737-800 with a cruise TSFC of 0.667 lb/lbf/hr. The resulting NASA 2019 ARMD target cruise TSFC is 0.3335 lb/lbf/hr [35].

Table 2 Specifications of S-curve models for turbofan cruise-specific fuel consumption given in Fig. 22.

	Practical Limit	**Theoretical Limit**	**2019 NASA ARMD**
Lower Asymptote (lb/lbf/hr)	0.353	0.299	0.3335
Upper Asymptote (lb/lbf/hr)	1	1	1
Inflection point (Year)	1981	1981	1981
Growth Rate	−0.0632	−0.0556	−0.0595
R square	0.5367	0.5264	0.5391

The inflection point year of 1981 was selected based on an interval of the most TSFC rapid improvement, identified

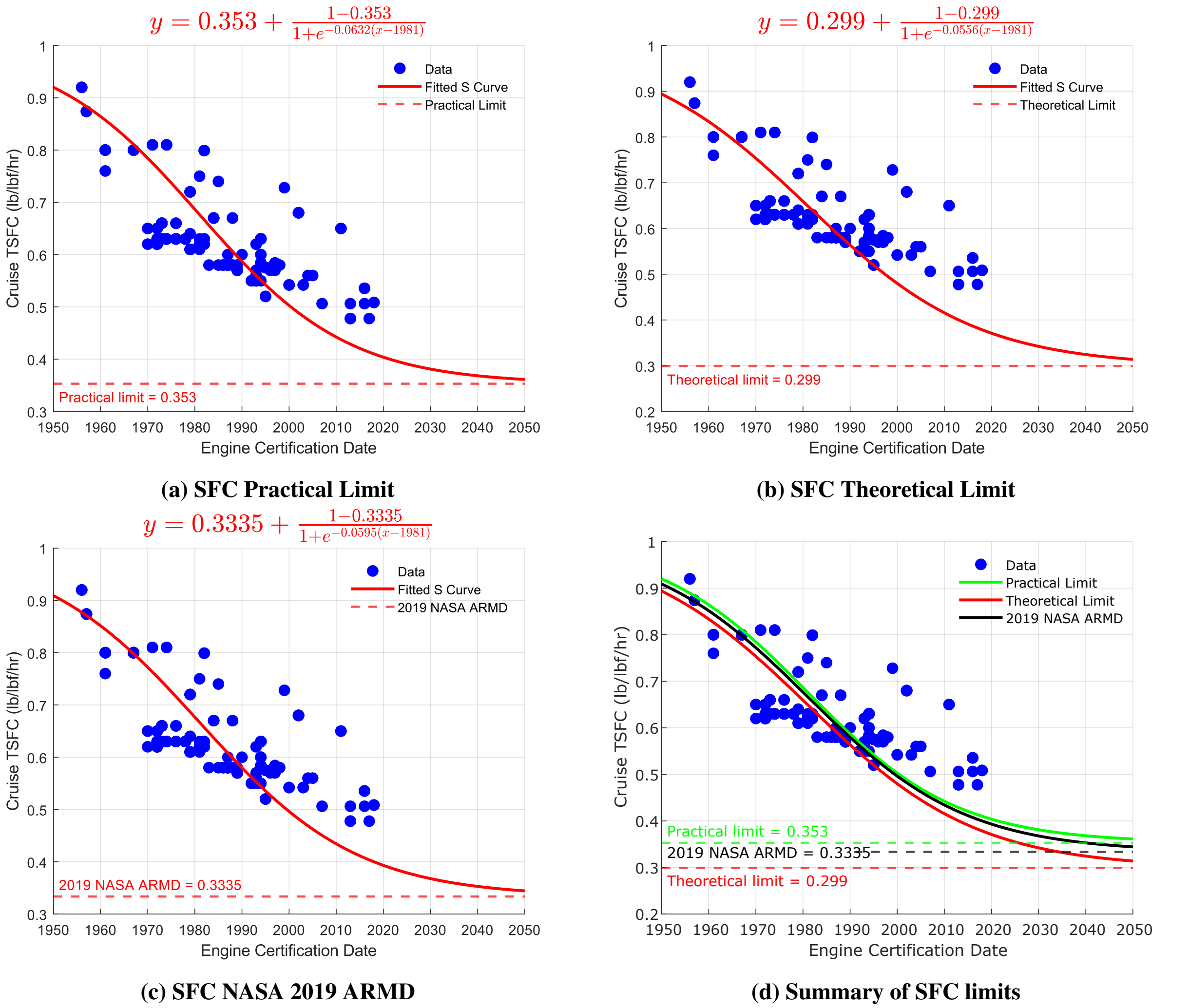

(a) SFC Practical Limit

(b) SFC Theoretical Limit

(c) SFC NASA 2019 ARMD

(d) Summary of SFC limits

Fig. 22 Comparison of thrust-specific fuel consumption projections based on practical limits, theoretical limits, and NASA 2019 ARMD estimates.

from data on 83 unique engines with available TCDS cruise TSFC information, this interval is between 1970 and 1990. This interval, spanning from 1970 to 1990, provided the strongest correlation with the S-curve projections. Then, the inflection year corresponding to the strongest R^2 with the S-curve was selected. Due to how conservative and aggressive the TSFC lower asymptote value is, the practical limit S-curve has the best R^2 value of 0.5367, and the theoretical limit S-curve has the lowest R^2 value of 0.5264. The NASA 2019 ARMD limit has an R^2 value in between those two at 0.5391.

These trends suggest that, from the available TCDS information on cruise TSFC, the current efficiency of high-bypass turbofan engines has entered a maturity phase, where advancements yield progressively smaller TSFC improvements. Achieving further substantial reductions in TSFC may therefore require radical propulsion technologies, such as ultra-high-bypass, open-rotor, or hybrid electric configurations, which may alter the theoretical limit and shift TSFC projections to a new S-curve, establishing a new efficiency baseline for future engines.

D. Lift-to-Drag Ratio (L/D)

Lift-to-drag ratio (L/D) is a primary performance parameter indicative of aerodynamic efficiency of an aircraft. While technological advancements are expected to enhance L/D, recent literature suggests that conventional tube-wing configurations may be approaching their practical efficiency limits. Warwick's findings align with this view, indicating that significant aerodynamic improvements with these configurations are increasingly unlikely [36].

Optimizing L/D involves a complex multidisciplinary design process, balancing aerodynamic shaping with structural and operational constraints. Efforts to overcome the aerodynamic efficiency limitations of traditional tube-wing designs have led to the exploration of novel wing-body configurations. These include Hybrid Wing Body (HWB) designs, such as NASA's ERA-224 and Boeing's BWB-0009A; Double-Bubble (DB) configurations, exemplified by MIT's D8; and Truss-Braced Wing (TBW) configurations, developed through Boeing's Subsonic Ultra Green Aircraft Research (SUGAR) program and NASA's X-66A.

In HWB configurations, Garmendia et al. [37] employed NASA-SC series supercritical airfoils for the outboard wing and vertical tail of the BWB-0009A, achieving a design lift coefficient (C_L) and cruise L/D of 23.02. In the DB configuration, Uranga et al. [38] at MIT conducted optimization studies focusing on boundary layer ingestion to reduce fuel burn, achieving a cruise L/D of 19.84 and a design C_L of 0.688 for the D8.2 model. For the TBW configuration, Ivaldi et al. [39] optimized the Boeing SUGAR TBW design through lift-constrained drag minimization, reaching a wing L/D of 25.33 at a design C_L of 0.75.

Enhancements in aerodynamic efficiency often focus on reducing drag through strategies such as minimizing surface area, reducing stability and control surface size, and managing laminar flow. Truss-braced wings, for example, are designed to maximize laminar flow by decreasing wing thickness-to-chord ratios, reducing Reynolds numbers, and wave drag. Additionally, unswept wings help mitigate spanwise flow disturbances, which facilitates laminar flow over larger wing regions. Structural constraints, such as maintaining minimum thickness-to-chord ratios, remain critical to sustain structural integrity [39].

1. Challenges in L/D Data Collection and Estimation Methods

A significant challenge in analyzing L/D trends is the limited availability of publicly accessible, reliable cruise L/D data from primary sources, such as manufacturers or regulatory bodies. While companies may maintain proprietary databases with such information, neither public records from FAA, EASA, nor manufacturers' data sheets typically disclose these values, necessitating estimation methods based on other available parameters.

This study applied three primary estimation methods:

- **Breguet Range Equation (BRE) Method:** Rearranged to solve for L/D using range, TSFC, cruise speed, and weight ratio:

$$\left.\frac{L}{D}\right|_{\text{Cruise}} = \frac{R * TSFC}{V_{\text{Cruise}} * \log \frac{1}{1-\frac{W_{\text{Fuel}}}{W_{\text{MTOW}}}}} \tag{8}$$

- **Weight-to-Thrust Ratio Method:** Assumes a balance of lift with weight and drag with thrust during cruise (i.e., steady state cruise). Cruise weight is approximated from MTOW, adjusted using takeoff and climb fuel fractions, following Raymer's formulation for transport aircraft [1]:

$$\left.\frac{L}{D}\right|_{\text{Cruise}} = \frac{W_{\text{Cruise}}}{T_{\text{Cruise}}} = \frac{W_{\text{MTOW}} * 0.995 * 0.985}{T_{\text{Cruise}}} \tag{9}$$

- **Mean Aerodynamic Chord (MAC) Method:** uses a regression model developed by Pasquale [40], which relates L/D to the aspect ratio (AR) and Reynolds number at the mean aerodynamic chord (Re_{mac}):

$$\left.\frac{L}{D}\right|_{\text{Cruise}} = 0.321 * \left(AR^2 Re_{mac}\right)^{3/16} \left(1 + 3.6AR^{-9/4}\right)^{-1/2} \tag{10}$$

where

$$Re_{mac} \approx 7.093 \times 10^6 c_{mac} M [1 - 0.5(z/23,500)^{0.7}] \tag{11}$$

Equation (11) is applicable to the range $3 \times 10^6 < Re_{mac} < 200 \times 10^6$ and atmosphere altitude range 0 < z < 50,000 ft. This regression is obtained from basic configuration data for 14 airplanes as listed in Pasquale [40].

Each method was applied using data from a publicly accessible database [11]. While individual sources in the database often included a maximum operating Mach number for various aircraft, they generally lacked information on a typical cruise Mach number, which is essential for the MAC method. To address this, a median cruise Mach number was estimated and applied for aircraft missing this data.

To ensure this assumption did not unduly influence the L/D estimates, a sensitivity analysis was conducted to examine how variations in the assumed cruise Mach number affected the average L/D. Cruise Mach was varied from 0.75 to 0.855, representing the observed range in the dataset. The results are shown in Fig. 23.

The sensitivity analysis in Fig. 23 shows that the mean L/D increases linearly with assumed Mach Number while the standard deviation remains constant. This indicates that although the assumed Mach number correlates with the L/D predicted by the MAC method, the effect is minimal relative to the variability in the dataset. Historically, cruise Mach numbers did increase as designers optimized transonic performance, particularly to manage drag divergence effects. However, subsonic cruise speeds have since reached a near-constant level due to physical constraints around the speed of sound and fuel efficiency considerations. Thus, for this analysis, a median cruise Mach number of 0.8 was selected to ensure consistent comparisons without introducing significant bias.

With this assumption in pace, sufficient data was available to apply the MAC method meaningfully across the dataset

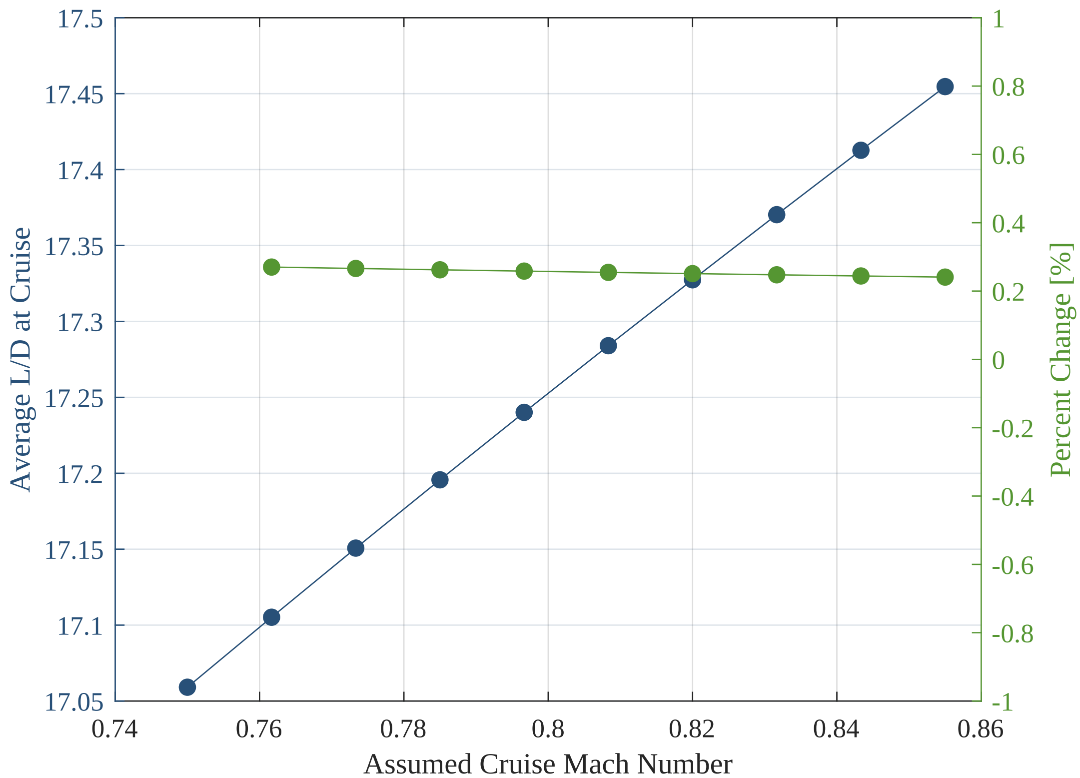

Fig. 23 Sensitivity of average database lift-to-drag ratio as a function of assumed cruise speed.

to predict the cruise L/D trends. Figure 24 presents L/D estimates derived using three methods across the historical database, showing distinct trends and variabilities for both single-aisle and double-aisle aircraft, with 90% confidence ellipses to indicate variability in each category.

The BRE method does not have sufficient data to draw conclusions in the single-aisle category. This is due to the lack of reliable cruise TSFC data in literature, which are required by this method. Predictions using BRE consistently fall below practical L/D values. This discrepancy likely stems from methodological assumptions about fuel weight and range. Since W_{Fuel} values from the database may represent maximum fuel capacity—including reserve fuel for diversion and holding—this could yield an overestimate of fuel weight relative to the actual mission fuel, resulting in lower L/D values. Additionally, typical commercial mission ranges reported in the data sources exclude reserve missions, causing a further imbalance.

The weight-to-thrust method has broader data coverage since it relies on more commonly available parameters in TCDS and APMs. However, these predictions also suffer from being unrealistic, showing a wide L/D range (12 to 24). This variability likely results from fuel fraction estimations used to approximate cruise weight. Unlike real flight conditions, where weight decreases continuously due to fuel burn, this method applies fixed weight fractions that cannot

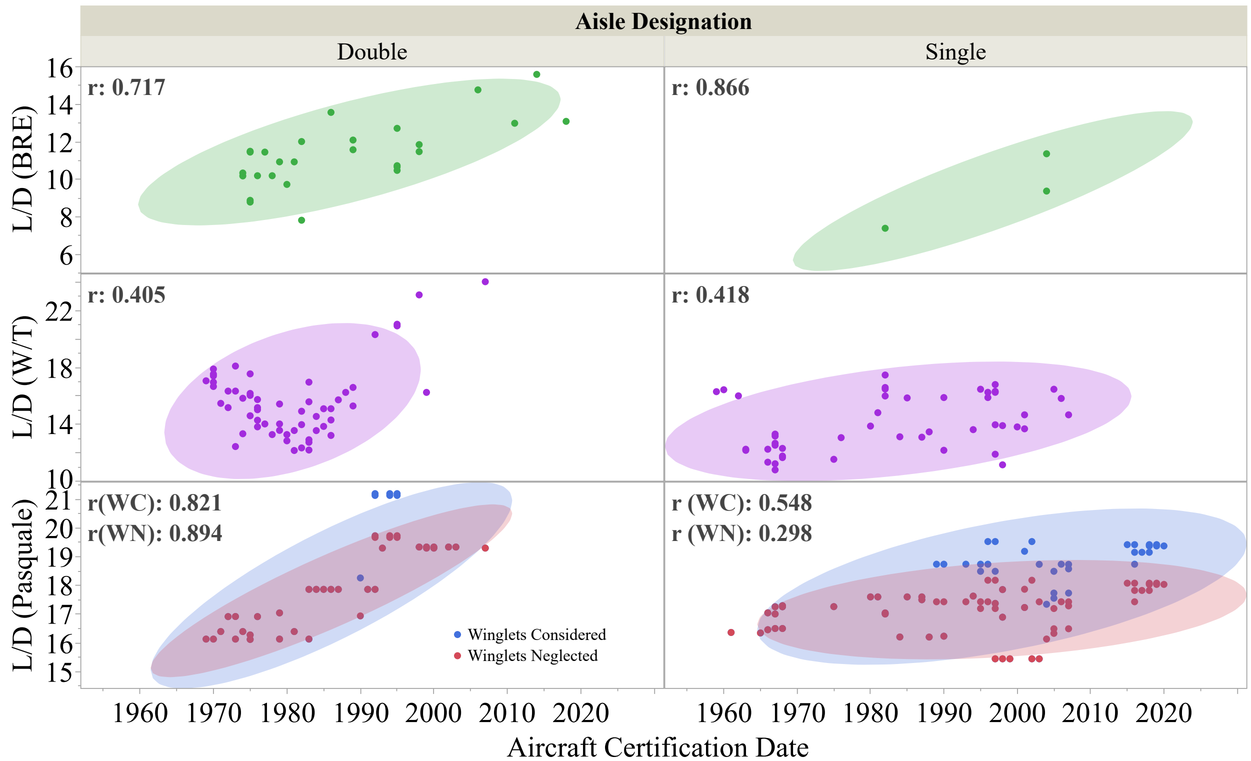

Fig. 24 Historical trends in lift-to-drag ratio for single-aisle and double-aisle aircraft, with 90% coverage ellipses to illustrate variability.

account for the dynamic nature of weight reduction during cruise. Therefore, while this method might be useful for capturing broader trends, its limitations in accuracy make it unsuitable for accurate historical L/D trend analysis.

Finally, the MAC method predicts L/D estimates within an intuitive range and with greater consistency across aircraft types. Its reliance of aspect ratio allows for a more accurate assessment of the effect of wing configuration changes over time, including the adoption of wingtip devices. Applying an effective aspect ratio increase of approximately 20% to account for wingtip devices (following Raymer's model [1]) aligns well with observed improvements in aerodynamic efficiency for single-aisle aircraft, where wingspan limitations have necessitated design optimizations. The resulting effect of the improved L/D for aircraft with winglets, using this method, is reflected in the trends shown in Figure 24, with color coding to distinguish configurations.

In summary, the MAC method emerges as the most reliable estimator for historical L/D trends, providing consistency and sensitivity to aerodynamic configurations over time. For future analysis, the W/T method could potentially be refined through more detailed fuel burn modeling. Meanwhile, the BRE method's limitations emphasize the importance of accurate mission-specific data inputs for estimating L/D, as general fuel and range assumptions can substantially skew results.

2. Factors Influencing L/D Trends

While L/D shows improvement over time, examining the trends of other aerodynamic parameters provides more information on the reasoning behind this phenomenon, and perhaps address some of the nuance of the evolution of L/D. Figure 25 illustrates the historical trends of key aerodynamic parameters, grouped by aisle count, with 90% coverage ellipses.

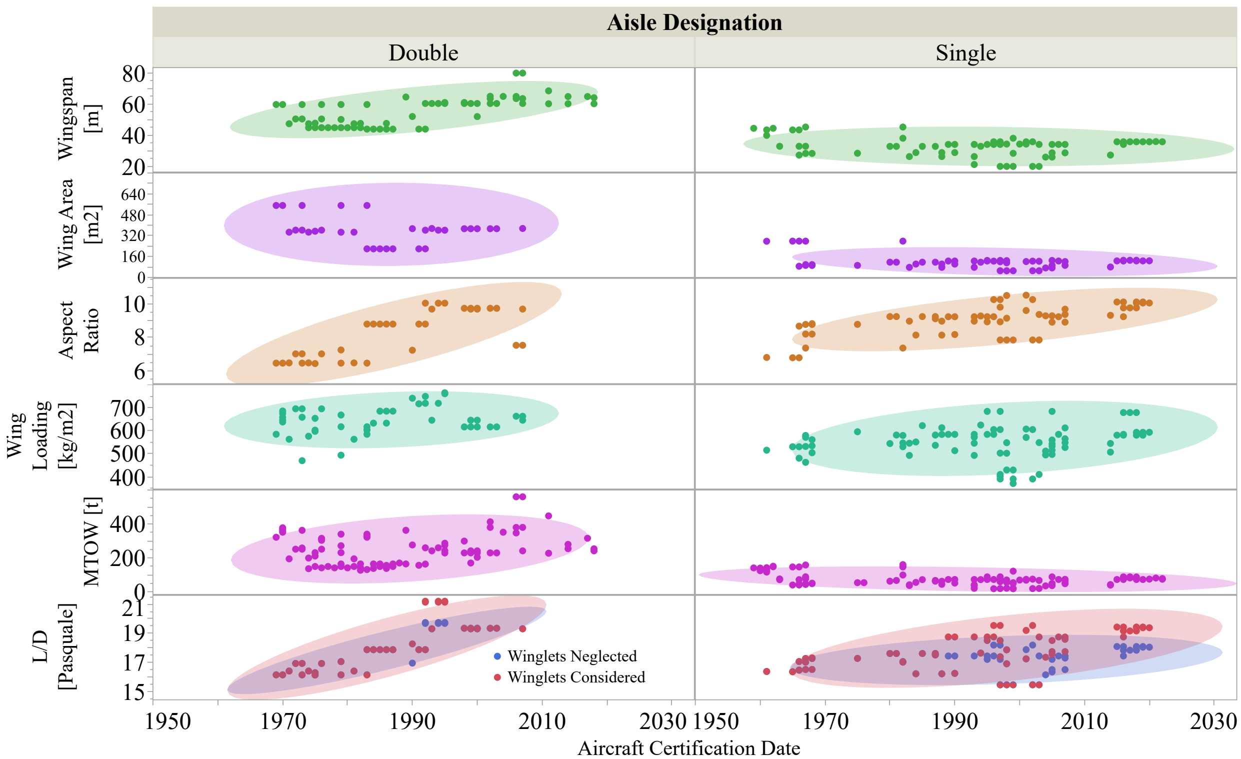

Fig. 25 Evolution of key aerodynamic parameters, grouped by aisle count, with 90% coverage ellipses showing trends over time.

With MTOW and wing loading (W/S) remaining largely constant over time, the wing area also shows minimal variation. This suggests that improvements in L/D arise primarily from optimizing the shape and configuration of the wing within a fixed area. In single-aisle aircraft, L/D gains appear more modest without the consideration of wingtip devices, reinforcing that these devices are a primary driver of L/D improvement after the 1990s.

This trend differs in double-aisle aircraft, where wingtip devices are less commonly employed as aerodynamic enhancers. The discrepancy is likely a consequence of regulatory limits on wingspan, which are stricter for single-aisle aircraft to ensure they fit within specific Aircraft Design Groups (ADGs). Figure 25 supports this interpretation, showing relatively constant wingspan trends in single-aisle aircraft, while double-aisle aircraft exhibit a gradual increase in wingspan. This pattern is consistent with Raymer's observations, where wingtip devices are only efficient when wingspan cannot be increased further due to design or regulatory constraints [1].

Looking forward, continued advancements in L/D are likely to follow these established trends. For single-aisle aircraft, improvements may focus on more advanced wingtip devices or innovative solutions like folding wings to work within ADG constraints. For larger aircraft, unrestricted by ADG limitations, more radical configurations such as BWB and TBW designs present promising avenues for future aerodynamic enhancement.

IV. Conclusions and Future Work

This work provides a comprehensive examination of historical trends and future projections of key performance parameters (KPPs) in commercial turbofan aircraft design. Drawing on an extensive database of over 400 commercial aircraft and 200 engines from authoritative sources such as FAA and EASA Type Certificate Data Sheets and manufacturers' specifications, this research offers a transparent and reliable foundation for KPP analysis.

The study examined four critical KPPs: operational empty weight to maximum takeoff weight ratio (OEW/MTOW), thrust-to-weight ratio (T/W), thrust specific fuel consumption (TSFC), and lift-to-drag ratio (L/D). These parameters represent structural efficiency, propulsion performance, and aerodynamic efficiency,essential to conceptual aircraft design and performance assessments.

The analysis revealed that changes in OEW/MTOW over time are influenced by a combination of factors, including aircraft range, size and maximum takeoff weight, and performance requirements. For double-aisle aircraft, decreasing OEW/MTOW trends correlate with increasing range and size rather than direct improvements in material technology. This indicates that using OEW/MTOW as a standalone metric for assessing structural advancements can be misleading without considering mission-specific design requirements. In contrast, the increasing OEW/MTOW trend in single-aisle aircraft was associated with higher engine weight fractions and additional weight from enhanced passenger comfort and safety features.

The T/W ratio was shown to be predominantly driven by performance requirements such as takeoff distance and climb rate rather than solely by technological advancements in engine performance. The data indicated that T/W has remained relatively stable for single-aisle aircraft and increased slightly for double-aisle aircraft due to evolving performance demands. Future projections suggests that significant changes in T/W are unlikely without a shift in design philosophy or mission requirements.

TSFC exhibited a clear downward trend over the past decades, strongly correlating with technological progress in engine efficiency. Applying S-curve modeling, the study projected that TSFC is approaching its practical lower limits with current turbofan technology, based on physical considerations like overall engine efficiency and environmental constraints. Substantial further reductions in TSFC may require adopting disruptive propulsion technologies such as ultra-high bypass ratio engines, open rotors, or hybrid-electric systems.

The analysis of L/D identified the mean aerodynamic chord-based approach as the most reliable for capturing aerodynamic trends. L/D has improved modestly over time, primarily due to aerodynamic refinements within the constraints of conventional tube-and-wing configurations. However, gains are increasingly challenging as designs approach practical aerodynamic efficiency limits. Future improvements in L/D may require unconventional configurations, such as hybrid wing bodies or truss-braced wings, which offer potential for substantial aerodynamic advancements.

This research contributed to the development of the Future Aircraft Sizing Tool (FAST), which integrates historical KPP trends to streamline initial aircraft design. As an open-source tool, FAST facilitates rapid exploration of design spaces with minimal inputs, leveraging a combination of physics-based and data-driven models. By embedding these historical KPP insights, this work provides aircraft designers and researchers with a robust, transparent resource for informed decision-making in early design stages.

In addition to its practical applications, the data-driven insights presented here offer educational value. While many discussions of aircraft performance trends address historical data in general terms, this study delineates the underlying physical drivers that shape these trends, allowing a clearer understanding of the nuanced interactions among KPPs, mission requirements, and technology advances.

In summary, this study highlights the complex relationships between technological advancements, performance requirements, and design constraints in aircraft development. Future research may expand the scope of KPPs and further explore their interactions with emerging technologies, such as electrified propulsion systems and advanced aerodynamic contributions.

Funding Sources

This work is sponsored by the NASA Aeronautics Research Mission Directorate and Electrified Powertrain Flight Demonstration project, “Development of a Parametrically Driven Electrified Aircraft Design and Optimization Tool”, WO-0238. Karin Bozak serves as NASA’s Technical Monitor.

Acknowledgments

The authors would like to thank Ralph Jansen, Amy Chicatelli, Andrew Meade, Karin Bozak, and Gaudy Bezos O’Connor from NASA’s Electrified Powertrain Flight Demonstration project for supporting this work and providing valuable technical input and feedback throughout the duration of the project.

References

[1] Raymer, D. P., *Aircraft design: A conceptual approach*, 4th ed., AIAA education series, American Institute of Aeronautics and Astronautics, Reston, Va., 2006. URL `http://www.loc.gov/catdir/toc/ecip068/2006004706.html`.

[2] Roskam, J., and Lan, C., *Airplane Aerodynamics and Performance*, Airplane design and analysis, Roskam Aviation and Engineering, 1997.

[3] Torenbeek, E., *Synthesis of Subsonic Airplane Design*, Delft University Press, Delft, 1982.

[4] Martinez-Val, R., Perez, E., and Palacin, J. F., "Historical evolution of air transport productivity and efficiency," *43 rd AIAA Aerospace Sciences Meeting and Exhibit*, 2005, p. 2005.

[5] Lee, J., "Historical and future trends in aircraft performance, cost, and emissions," *Massahusettes Institute of Technology*, 2000.

[6] Ballal, D. R., and Zelina, J., "Progress in aeroengine technology (1939–2003)," *Journal of aircraft*, Vol. 41, No. 1, 2004, pp. 43–50.

[7] Martinez-Val, R., Palacin, J., and Perez, E., "The evolution of jet airliners explained through the range equation," *Proceedings of the Institution of Mechanical Engineers, Part G: Journal of Aerospace Engineering*, Vol. 222, No. 6, 2008, pp. 915–919.

[8] Martinez-Val, R., and Perez, E., "Aeronautics and astronautics: recent progress and future trends," *Proceedings of the Institution of Mechanical Engineers, Part C: Journal of Mechanical Engineering Science*, Vol. 223, No. 12, 2009, pp. 2767–2820.

[9] Lee, J. J., Lukachko, S. P., Waitz, I. A., and Schafer, A., "Historical and future trends in aircraft performance, cost, and emissions," *Annual Review of Energy and the Environment*, Vol. 26, No. 1, 2001, pp. 167–200.

[10] Babikian, R., Lukachko, S. P., and Waitz, I. A., "The historical fuel efficiency characteristics of regional aircraft from technological, operational, and cost perspectives," *Journal of Air Transport Management*, Vol. 8, No. 6, 2002, pp. 389–400. https://doi.org/https://doi.org/10.1016/S0969-6997(02)00020-0, URL https://www.sciencedirect.com/science/article/pii/S0969699702000200.

[11] IDEAS Laboratory, "Future Aircraft Sizing Tool (FAST)," , 2024. URL https://github.com/ideas-um/FAST.

[12] Duffy, K. P., and Jansen, R. H., "Turboelectricand hybrid electric aircraft drive key performance parameters," *2018 AIAA/IEEE Electric Aircraft Technologies Symposium (EATS)*, IEEE, 2018, pp. 1–19.

[13] Jansen, R., Duffy, K. P., and Brown, G., "Partially turboelectric aircraft drive key performance parameters," *53rd AIAA/SAE/ASEE joint propulsion conference*, 2017, p. 4702.

[14] Jansen, R., Brown, G. V., Felder, J. L., and Duffy, K. P., "Turboelectric aircraft drive key performance parameters and functional requirements," *51st AIAA/SAE/ASEE joint propulsion conference*, 2015, p. 3890.

[15] Pastra, C. L., Hall, C., Cinar, G., Gladin, J., and Mavris, D. N., "Specific power and efficiency projections of electric machines and circuit protection exploration for aircraft applications," *2022 IEEE Transportation Electrification Conference & Expo (ITEC)*, IEEE, 2022, pp. 766–771.

[16] Hall, C., Pastra, C. L., Burrell, A., Gladin, J., and Mavris, D. N., "Projecting power converter specific power through 2050 for aerospace applications," *2022 IEEE Transportation Electrification Conference & Expo (ITEC)*, IEEE, 2022, pp. 760–765.

[17] Tiede, B., O'Meara, C., and Jansen, R., "Battery key performance projections based on historical trends and chemistries," *2022 IEEE Transportation Electrification Conference & Expo (ITEC)*, IEEE, 2022, pp. 754–759.

[18] Roux, E., *Turbofan and Turbojet Engines: Database Handbook*, Éditions Élodie Roux, 2007.

[19] Roux, E., *Turboshaft, Turboprop and Propfan: Database Handbook*, Éditions Élodie Roux, 2011.

[20] *Janes All the World's Aircraft: In service 2022-2023*, Jane's group UK limited., 2022. URL https://books.google.com/books?id=bw_yzgEACAAJ.

[21] Administration, F. A., "Aircraft Characteristics Data," , 2023. Data retrieved from FAA, https://www.faa.gov/airports/engineering/aircraft_char_database/data.

[22] Eurocontrol, "Aircraft Performance Database," , n.d. URL https://contentzone.eurocontrol.int/aircraftperformance/default.aspx.

[23] Jenkinson, L., Simpkin, P., and Rhodes, D., "Civil Jet Aircraft Design Data Sets," , 2001. URL https://booksite.elsevier.com/9780340741528/appendices/default.htm.

[24] Arnson, M., Aljaber, R., and Cinar, G., "Predicting Aircraft Design Parameters using Gaussian Process Regressions on Historical Data," *AIAA SciTech 2025 Forum*, 2025. This paper is submitted for publication at SciTech Forum 2025.

[25] Rashid, M., Sarkar, J., and Phuyal, S., "Visualizing Bivariate Statistics Using Ellipses Over a Scatter Plot," 2022.

[26] JMP, "Confidence Ellipse," https://www.jmp.com/support/help/en/18.0/index.shtml#page/jmp/ellipse.shtml, 2024. Accessed: 2024-09-05.

[27] Cleveland, F. A., "Size effects in conventional aircraft design," *Journal of Aircraft*, Vol. 7, No. 6, 1970, pp. 483–512.

[28] Torenbeek, E., *Advanced aircraft design: conceptual design, analysis and optimization of subsonic civil airplanes*, John Wiley & Sons, 2013.

[29] Lee, C., Salit, M. S., Hassan, M., et al., "A review of the flammability factors of kenaf and allied fibre reinforced polymer composites," *Advances in Materials Science and Engineering*, Vol. 2014, 2014.

[30] Mattingly, J. D., *Aircraft engine design*, Aiaa, 2002.

[31] Kellari, D., Crawley, E. F., and Cameron, B. G., "Influence of technology trends on future aircraft architecture," *Journal of Aircraft*, Vol. 54, No. 6, 2017, pp. 2213–2227.

[32] NASA Glenn Research Center, "Specific Fuel Consumption (SFC)," https://www.grc.nasa.gov/www/k-12/airplane/sfc.html, 2021. Accessed: 2024-11-05.

[33] National Academies of Sciences, Engineering, and Medicine, *Commercial Aircraft Propulsion and Energy Systems Research: Reducing Global Carbon Emissions*, National Academies Press, 2016.

[34] Singh, R., Ameyugo, G., and Noppel, F., "Jet engine design drivers: past, present and future," *Innovation in Aeronautics*, Elsevier, 2012, pp. 56–82.

[35] National Aeronautics and Space Administration, "NASA Aeronautics Strategic Implementation Plan: 2019 Update," http://www.nasa.gov, 2019. NASA Aeronautics Research Mission Directorate.

[36] Warwick, G., "Future Shaping," *Aviation Week & Space Technology*, Vol. 172, No. 20, 2010, pp. 40–42. URL https://archive.aviationweek.com/issue/20100517.

[37] Garmendia, D. C., Chakraborty, I., and Mavris, D. N., "Method for evaluating electrically actuated hybrid wing–body control surface layouts," *Journal of Aircraft*, Vol. 52, No. 6, 2015, pp. 1780–1790.

[38] Uranga, A., Drela, M., Greitzer, E. M., Hall, D. K., Titchener, N. A., Lieu, M. K., Siu, N. M., Casses, C., Huang, A. C., Gatlin, G. M., et al., "Boundary layer ingestion benefit of the D8 transport aircraft," *AIAA journal*, Vol. 55, No. 11, 2017, pp. 3693–3708.

[39] Ivaldi, D., Secco, N. R., Chen, S., Hwang, J. T., and Martins, J. R., "Aerodynamic shape optimization of a truss-braced-wing aircraft," *16th AIAA/ISSMO multidisciplinary analysis and optimization conference*, 2015, p. 3436.

[40] Sforza, P. M., "Direct Calculation of Zero-Lift Drag Coefficients and (L/D)max in Subsonic Cruise," *Journal of Aircraft*, Vol. 57, No. 6, 2020, pp. 1224–1228. https://doi.org/10.2514/1.C035717, URL https://doi.org/10.2514/1.C035717.